DESIGN AND ANALYSIS OF A COMPOSITE BEAM FOR SIDE IMPACT PROTECTION OF A SEDAN

A Thesis by

Divakara H Basavaraju

Bachelor of Engineering, Mysore University, India, 1998

Submitted to the Department of Mechanical Engineering
and the faculty of the Graduate School of
Wichita State University
in partial fulfillment of
the requirements for the degree of
Master of Science

December 2005

DESIGN AND ANALYSIS OF A COMPOSITE BEAM FOR SIDE IMPACT PROTECTION OF A SEDAN

The following faculty members have examined the final copy of this copy of thesis for form and content and recommend that it be accepted in partial fulfillment of the requirements for the degree of Master of Science, with a major in Mechanical Engineering.

_____
Hamid M. Lankarani, Committee Chair

_____
Babak Minaie, Committee Member

_____
Krishna K. Krishnan, Committee Member

DEDICATION

To My Parents

ACKNOWLEDGEMENTS

I would like to take this opportunity to thank my research advisor Dr. Hamid M. Lankarani for his help and guidance.I also wish to thank my committee members Dr. Behnam Bahr and Dr. Krishna K. Krishnan for being part of the committee and going through this report and making valuable suggestions.

Special thanks to Tiong Keng Tan and Kim Leng of National Institute for Aviation Research for supporting me financially throughout my Master's degree. Without their extended help I would not be finishing the Master's degree at the right time.

I am indebted to my colleagues at the Computational Mechanics Laboratory for their help, support, and kind cooperation in the completion of this thesis. Special thanks to Aniruddha Deo, Vikram Krishnamurthy, Ashwin Sheshadri and Kumar Nijagal Honnagangaiah.

Finally, I would like to thank my parents, family, roommates and other friends who were involved directly or indirectly in completion of my thesis.

ABSTRACT

Side Impact crashes can be generally dangerous because there is no room for large deformation to protect an occupant from the crash forces. The side impact collision is the second largest cause of death in United States after frontal crash. Day by day increase in the fuel cost and the emission of the smoke from the automobile industry are also the major concerns in the contemporary world, hence the safety, fuel efficiency and emission gas regulation of the passenger cars are important issues in contemporary world. The best way to increase the fuel efficiency without sacrificing the safety is to employ composite materials in the body of the cars because the composite materials have higher specific strength than those of steel. Increase in the usage of composite material directly influences the decrease in the total weight of car and gas emission. In this research, Carbon/Epoxy AS4/3051 -6 is used as material for side impact beam which has adequate load carrying capacities and that it absorbs more strain energy than steel.

The Finite Element models of a Ford Taurus car and the Moving Deformable barrier (MDB) as developed by National Crash Analysis Center (NCAC) have been utilized for the analysis in this thesis. The current side impact beam is removed from the car and the new beam which is developed using CATIA and MSC.Patran is merged on to the driver side of the front door of the car model.

The total energy absorption of the new beam with steel and composite material is compared with the current beam. The intrusion of the beam is evaluated by using FMVSS 214 and IIHS side impact safety methods. The new impact beam with composite has high impact energy absorption capability when compared to current beam and new beam with steel, with 65% reduction in weight.

TABLE OF CONTENTS

CHAPTER **PAGE**

1. INTRODUCTION 1

1.1 Background…… ……..1
1.2 NHTSA/Crashworthiness 3
1.3 Federal Motor Vehicle Safety Standard (FMVSS 214) 4
1.4 Insurance Institute for Highway Safety, Side Impact Test Protocol 6
1.5 Objective 7

2. LITERATURE REVIEW 9

2.1 Requirements of Side Impact Beam 9
2.2 Side Impact Protection 10
2.3 Energy Absorption Capability of Composites 11
2.4 Carbon Fiber Composites in Automobile Parts 12

3. C.A.E TOOLS 14

3.1 CATIA V5 14
3.2 MSC Patran 14
3.3 LS-DYNA 15
3.4 EASI CRASH DYNA (ECD) 16

4. MODELING AND ANALYSIS OF THE IMPACT BEAM 18

4.1 Design of the Side Door Impact Beam 18
4.2 Comparison of Current Beam with New Beam 20
4.3 Material Description 20
4.4 Beam Modeling 21
4.5 Modeling of Impact Body 23
4.6 Current Impact Beam 24
4.7 Optimization of the Composite Impact Beam 25
4.8 Comparison of Beam at Different Impact Angles 26
4.9 Weight Comparison 27
4.10 Comparative Analysis of Impact Beam 27
4.11 Energy Absorption 29
4.11.1 Comparison between new beam with the current beam 29
4.11.2 Composite beam with steel beam 30
4.12 Total Energy Absorption 31

5. SIDE IMPACT MODELING 32

5.1 Finite Element Model of Ford Taurus 32
5.2 Impactor Modeling 34

6. RESULTS AND DISCUSSION 37

TABLE OF CONTENTS (Continued)

CHAPTER **PAGE**

6.1 FMVSS 214 Test Configuration 37
6.1.1 Simulation results with current side impact beam 38
6.1.2 Simulation results with new steel side impact beam 40
6.1.4 Intrusion of the beam 41
6.1.6 Comparison of new beam with steel and composite 43
6.2 Insurance Institute for Highway Safety (IIHS) Side Impact Test Configuration. 44
6.2.1 Comparison of current steel beam with new steel beam 46
6.2.2 Comparison of new steel beam with composite beam 47

7. CONCLUSIONS AND RECOMMENDATIONS 49

REFERENCES 51

APPENDIX 54

LIST OF TABLES

TABLE **PAGE**

Table 1: Material Properties for Carbon Fiber Laminate 21

Table 2: Material Property for Steel 21

Table 3: Beam Model Summery 22

Table 4: Impactor Model Summary 23

Table 5: Summary of Composite Beam under Impact Loading 25

Table 6: Energy Absorption of Composite Beam for Different Impact Angles 27

Table 7: Side Impact Beam Weight 27

Table 8: Total Energy Absorption of Side Impact Beam 31

Table 9: Model Summary of Ford Taurus Car 33

Table 10: Material Properties of Ford Taurus Car 34

Table 11: Model Summary of Moving Deformable Barrier 35

LIST OF FIGURES

FIGURE **PAGE**

Figure 1: Door with Side Impact Beam 2

Figure 2: FMVSS 214 Test Configuration [1] 5

Figure 3: IIHS Test Configuration [3] 6

Figure 4: Methodology 8

Figure 5: Injury Pattern in Side Impact [4] 10

Figure 6: Specific Energy of Different Materials [11] 12

Figure 7: Dimensions of Side Impact Beam 19

Figure 8: Side Impact Beam 22

Figure 9: Side Impact Beam with Mesh 22

Figure 10: Impactor 23

Figure 11: Current Side Impact Beam with Door 24

Figure 12: Current Side Impact Beam 24

Figure 13: Force Displacement Curve for Different Fiber Orientation and Thickness 25

Figure 14: Force Displacement Curve for Different Impact Angles 26

Figure 15: New Side Impact Beam before Impact 28

Figure 16: New Side Impact Beam after Impact 28

Figure 17: Current Side Impact Beam before Impact 28

Figure 18: Current Side Impact Beam after Impact 29

Figure 19: New Side Impact Composite Beam after Impact 29

Figure 20: Force Displacement curves for New and Current Beam 30

Figure 21: Force Displacement Curve for Steel and Composite 31

LIST OF FIGURES (Continued)

FIGURE **PAGE**

Figure 22: Finite Element Model of Ford Taurus 34

Figure 23: Finite Element Model of Moving Deformable Barrier 35

Figure 24: Moving Deformable Barrier Face [1] 36

Figure 25: Dimensions of Moving Deformable Barrier [1] 36

Figure 26: FMVSS 214 Test Configuration [1] 37

Figure 27: Side Impact Model of Ford Taurus car 38

Figure 28: Car Model after Impact 39

Figure 29: Acceleration at Center of Gravity of the Car 39

Figure 30: Car Model with New Impact Beam after Impact 40

Figure 31: New side Impact Beam after Impact 40

Figure 32: Acceleration at Center of Gravity 41

Figure 33: Intrusion of Beam with Steel 42

Figure 34: Acceleration of the Beam with Steel 42

Figure 35: Intrusion of New Beam 43

Figure 36: Acceleration of New Beam 44

Figure 37: IIHS Side Impact Test Configuration [3] 45

Figure 38: Side Impact Model for Ford Taurus Car 45

Figure 39: Intrusion of Steel Impact Beam 46

Figure 40: Acceleration of Steel Impact Beam 46

Figure 41: Intrusion of New Impact Beam 47

Figure 42: Acceleration of New Impact Beam 47

CHAPTER 1

INTRODUCTION

1.1 Background

Crashworthiness is the ability of the vehicle structure to sustain impact loading and to prevent the occupant injuries at the time of accidents. Side impact crash is generally dangerous, since there is no room for large deformation of the vehicle structures. In United States side impacts is the second most common type of vehicle impacts after frontal impact that results in injuries to occupants which account to 25 percent of fatalities due to impacts between passenger cars and light trucks and approximately 30 percent between passenger car crashes [1].

The fuel efficiency and gas emission regulation of the passenger are also very important in the contemporary world. Every day the price of the fuel and the requirement of the fuel is increasing randomly, eventually emission of chemicals from the vehicle exhaust pollute the environment and increase the global temperature.

Therefore the safety and gas emission regulation of passenger car are very important issues in automotive industry. They directly impact the final vehicle design. The manufacturers meet the requirements of a particular crashworthiness standard and fuel efficiency by making the approximate design change in their vehicle structure and by introducing necessary structural components that satisfy the overall design objectives.

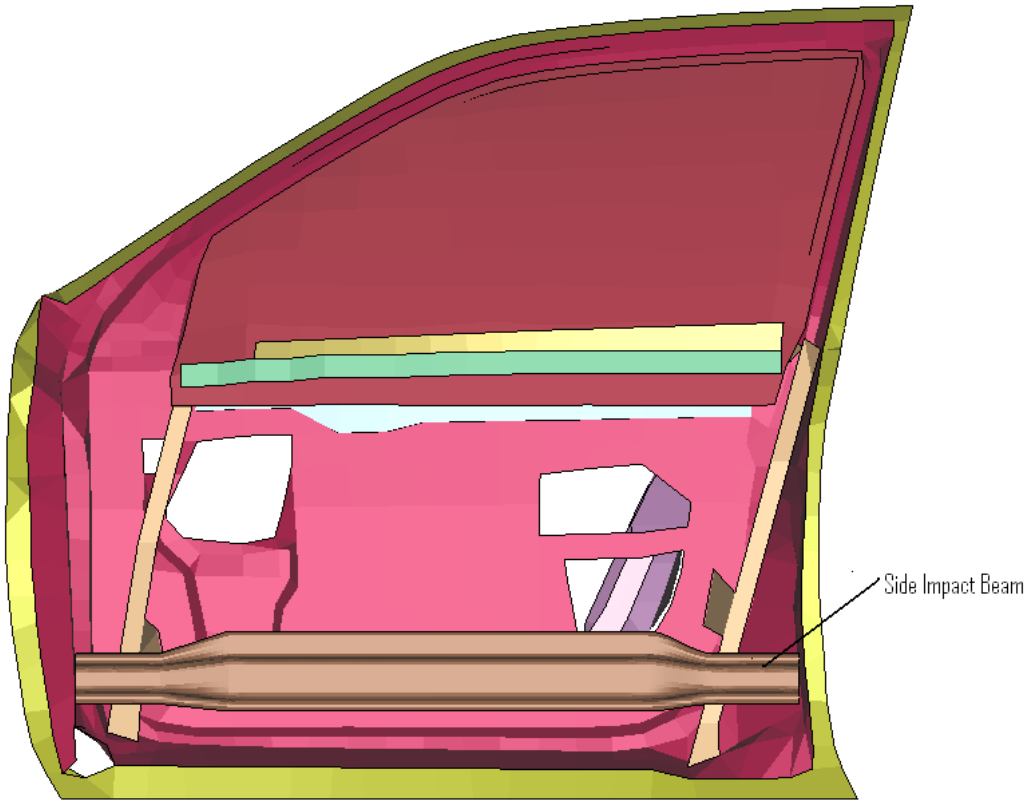

Figure 1: Door with Side Impact Beam

The present vehicle standard requires each door to resist crash forces that are applied by loading cylinder. The manufacturers are generally required to meet the requirement of the side door strength by reinforcing the doors with door beams (intrusion beam). The main function of the side-impact beam is to provide the occupant with a high level of safety. Side Impact beam is fitted to the inside of car door in the lower third of the door frame and designed to minimize the passenger compartment penetration in the event of side crash.

Stiffness of the material plays a major role in optimal design of side door structures. The intrusion of the side door structure should be minimal and the force exerted on the side door during the crash must be distributed over the surface in such a way that the passenger in the structural cage is affected as little as possible. In regard to these directions FMVSS

214 of American standard NHTSA should be taken into consideration when designing the side door impact beams.

Composite materials have been used in aircraft and space vehicles as they have high specific strength (Strength/Density), high specific stiffness (Stiffness/Density) and very good fatigue properties. With the composite material the designer can vary structural parameters, such as geometry and at the same time vary the material properties by changing the fiber orientation, fiber content. These properties of the composite materials create the auspicious environment in automobile industries, since they provide required strength for less weight when compared to steel and aluminum.

Carbon fiber reinforced composites are known for their high impact energy absorption characteristics. The carbon fiber composite have very high specific strength and specific stiffness. The car body made of carbon fiber composites bring about an increase in fuel efficiency, reduction in atmospheric pollution and human body injuries when accidents occur.

1.2 NHTSA/Crashworthiness

The U.S. Department of Transportation established National Highway Traffic Safety Administration (NHTSA) under Highway Safety Act of 1970. The NHTSA is a successor to the National Highway Safety Bureau, to conduct safety programs under the National Traffic and Motor Vehicle Safety Act of 1966 and the Highway Safety Act of 1966. The United States Code under Title 49 outlines in Chapter 301, Motor Vehicle Safety the requirements for manufacturers and items of motor vehicles. The NHTSA also conducts various consumer programs, which are outlined in various Chapters under Title 49 established by the Motor Vehicle Information and Cost Savings Act of 1972.

The major goal of NHTSA is to save lives, prevent injuries and reduce economic costs resulting from vehicle crashes. This goal is achieved by establishing and enforcing safety standards for motor vehicles manufacturers and through government awareness programs which help conduct effective local highway safety programs. NHTSA is also constantly monitors and investigates of new safety standards which help to minimize the casualties caused by the motor crashes and implements these new safety standards.

The NHTSA is in constant investigation of safety defects in motor vehicles, formulates and enforces fuel economy standards, helps of government and local organization to minimize the risk of drunk drivers. Sets the standard and promote the use of child safety seats and seat belts, establish vehicle anti-theft regulations. In order to bring effective safety improvements NHTSA conducts research on driver behavior and traffic safety.

1.3 Federal Motor Vehicle Safety Standard (FMVSS 214)

Side Impact Protection was amended in 1990 under the Federal Motor Vehicle Safety Standard (FMVSS) 214 to guarantee the occupant protection in a crash test that simulates a serious perpendicular collision. Since the Side Impact caused 33 percent of fatal injuries in 1993 to passenger car occupants, it was manifested to new passenger car models during the year 1994 to 1997. It is among the most critical and promising safety regulation circulated by the National Highway Traffic Safety Administration (NHTSA).

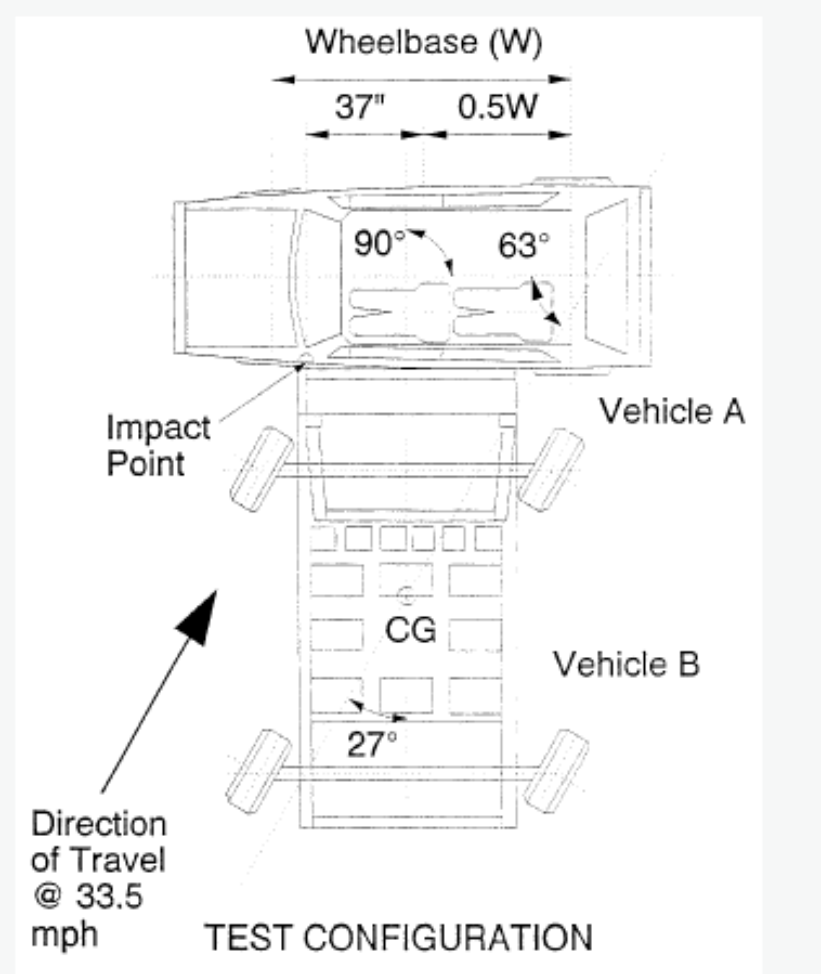

Figure 2: FMVSS 214 Test Configuration [1]

The present FMVSS 214 is the outcome of many years of research to manufacture the passenger vehicle less susceptible to Side Impacts, and mainly to reduce casualty to the nearside occupant during the vehicle struck by another vehicle near door area, which is primary responsible for the majority of side-impact casualties. With the combined effort from United States and International communities, NHTSA developed

- A test methodology to determine the severity of intersection collision between two vehicles using a Moving Deformable Barrier (MDB).

- Thoracic Trauma Index (TTI), which determines the severity of thoracic injuries when occupant's torsos contact the interior side member of a car.
- A Side Impact Dummy (SID) on which Thoracic Trauma Index (TTI) can be measured with required accuracy during Side Impact Tests. This injury score measured called TTI (d).
- The TTI (d) up to 90 in 2-door cars and 85 in 4- door cars is allowed under new FMVSS 214.

The Government Performance and Results Act of 1993 and Executive Order 12866 mandate all automobile manufacturers and agencies to evaluate their existing programs and regulations. The main objective of this evaluation is to determine the actual benefits – lives saved, injuries avoided and damages prevented – and the feasibility of safety equipment installed in production vehicles in connection with a rule.

1.4 Insurance Institute for Highway Safety, Side Impact Test Protocol

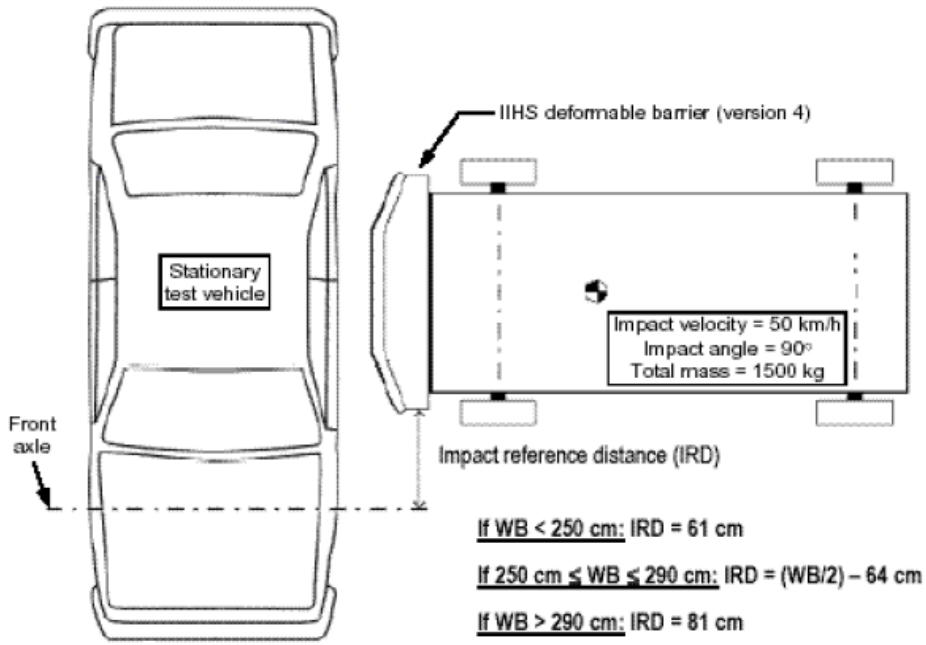

Figure 3: IIHS Test Configuration [3]

The Institute's side impact test is relatively very severe. Given the design of today's vehicles, it's unlikely that people in real world crashes, as severe as this test would emerge uninjured. But with good side impact protection, people should be able to survive crashes of this severity without serious injuries.

In this test procedure the crash is similar to the one used in Federal Motor Vehicle Safety Standard (FMVSS 214) but the wheels on the moving deformable barrier(MDB) are aligned with the longitudinal axis of the cart(zero degrees) to allow for 90 degree impact with velocity of 50 Kmph (31 mph) [3].

1.5 Objective

The main object of this research work is to replace the current side impact beam with the better design and using a composite material instead of steel in order to reduce the total weight of the car without sacrificing the safety of the passenger. Therefore in this study in accordance with the basic principles of crashworthiness which state that the intrusion of the striking vehicle should be minimum and the energy absorbing capability of the deforming structure should be high, the usage of the composite side impact beams on the car door has been proposed and its effectiveness in reducing intrusion has been evaluated.

Methodology

This thesis begins with the development of the better designed side impact beam, then comparing the new steel beam with a current steel beam for total energy absorption. The material property of the new beam is changed from steel to carbon fiber composite. The material orientation and thickness of the composite beam is found out by finding the total energy absorption and peak load.

Effectiveness of the current steel beam, new steel beam and new beam with composite material is found out by finding the intrusion and acceleration at the center of the beam by implementing them into the finite element model of Ford Taurus car and tested according to the FMVSS 214 and IIHS.

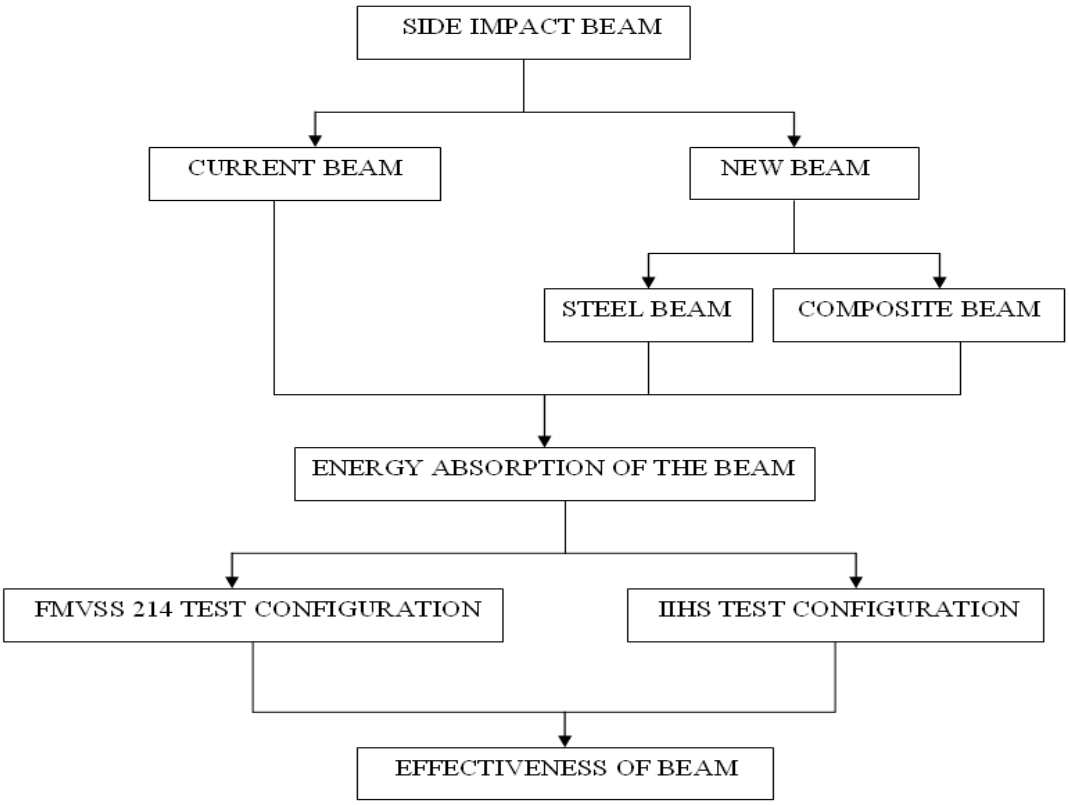

Figure 4: Methodology

CHAPTER 2

LITERATURE REVIEW

Previous studies by different researches show that the efficient design and increase use of composite materials into the automotive parts directly influences the car safety, weight reduction and gas emission, because the efficient design can absorb more deformation and composite materials have high specific strength (strength to density) and high specific stiffness (stiffness/density). They also have very high impact load absorbing and damping properties.

2.1 Requirements of Side Impact Beam

Federal Motor Vehicle Safety Standards (FMVSS) No. 214 establishes the minimum strength required for side doors of passenger cars. The side doors must be able to withstand 0an initial crush resistance of at least 2,250 pounds after 6 inches of deformation, and intermediate crush resistance of at least 3,500 pounds(without seats installed) or 4,375 pounds(with seats installed)after 12 inches of deformation and a peak crush resistance of two times the weight of the vehicle or 7,000 pounds whichever is less(without seat installed) or 3-1/2 times the weight of the vehicle or 12,000 ponds whichever is less(with seats installed) after 18 inches of deformation [1].

The major factors in considering the materials for the side door are load path and maximum resisting load of the door. The load carrying capacity and intrusion of the side door structure mainly depends on mechanical properties, shape, size and thickness of its components. The proper combination of these features can dramatically change the behavior of the structure, providing an efficient design [8].

The side impact beam should have the ability to absorb as much deformational energy as possible without breaking. Steel is still the most widely used material for beam members, but the steel increases the total weight of the car. However, breakthroughs in the application of lighter materials, such as composite, are being initiated in the automotive industry. Correct fiber orientation and stacking sequence of the cross-ply laminate contribute to higher energy absorption when compared to steel equivalent.

The impact beams normally have large static strength and high impact energy absorption capability, which properties are seldom possessed simultaneously by conventional metals because usually metals with high strength have low toughness and vice versa. To meet the high strength and high toughness properties, impact beams are made up of high strength alloy steel with several heat treatments. However the steel impact beams increase the weight of the car and the heat treated steel impact beam usually has a low nil-ductility temperature. The best way to reduce the structural weight of the impact beam is to employ the composite materials as fiber reinforced composite materials have very high specific strength.

2.2 Side Impact Protection

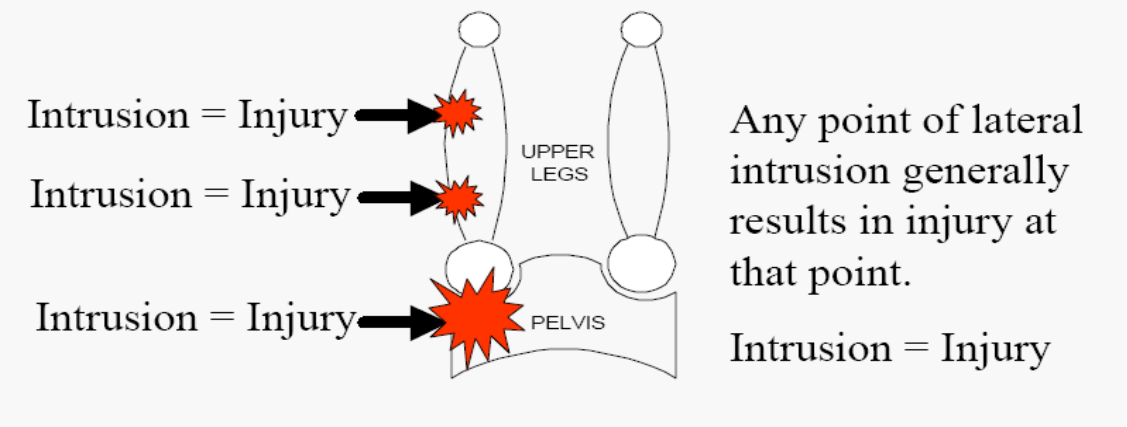

Figure 5: Injury Pattern in Side Impact [4]

Intrusion most commonly increases the risk of chest, abdominal and pelvic injuries [4]. Door panel intrusion is still the most significant contributor in occupant injuries. Before the implementation of the side impact standard, it was likely that the lower door panel would intrude and result in pelvic fracture. The stiffness, geometry and intrusion of door panels in side impact result in specific injury patterns.

In order to avoid the side door intrusion into the passenger car compartment, the vehicle manufacturers generally reinforce the side doors with intrusion beams.

2.3 Energy Absorption Capability of Composites

The energy absorption capability [8], [9], [10] of the composite structure mainly depends on the

- Fiber Material – Physical properties of the fiber material directly influences the specific energy absorption of the composite. The brittle nature of the fiber results in more energy absorption rather than the ductile nature of the fiber, which fails by progressive folding.
- Matrix Material – Specific energy absorption linearly increases with the matrix compressive strength.
- Fiber and Matrix Combination – Due to crushing by high energy fragmentation, matrix material with a higher failure strain has high energy absorption than the fiber material.
- Fiber Orientation and Lay-up – High energy absorption composites consist of layers of specified orientation and sequence plies.

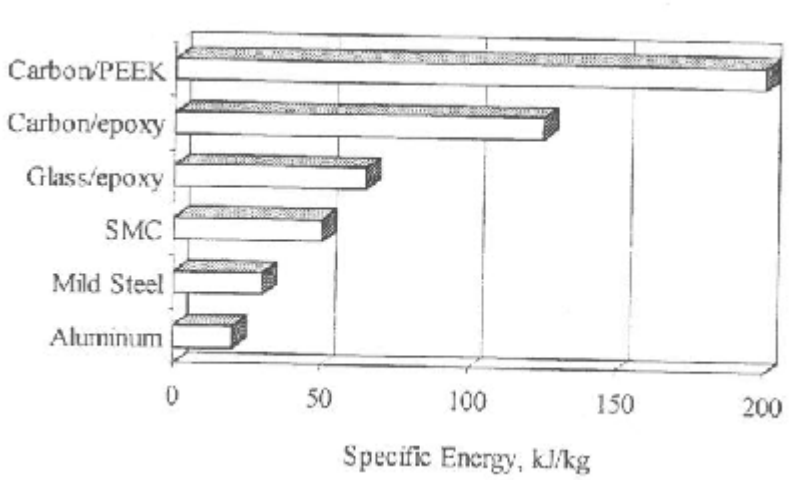

Figure 6: Specific Energy of Different Materials [11]

The composite materials have high specific energy absorption when compared to steel. The properties like high specific strength and high specific stiffness are attractive for the construction of lightweight and fuel efficient vehicle structures. The energy absorption capability of the composite materials offers a unique combination of reduced weight and improves crashworthiness of the vehicle structures [11].

2.4 Carbon Fiber Composites in Automobile Parts

Fuel efficiency of the vehicle directly depends on the weight of the vehicle. The carbon fiber composite body structure is 57% lighter than steel structure of the same size and providing the superior crash protection, improved stiffness and favorable thermal and acoustic properties [12].

The composite materials are replacing most of the steel structures. Rotors manufactured using RTM (Resin Transfer Molding) for air compressor or super chargers of cars are used to substitute for metal rotors which are hard to manufacture [4].

The composite material was for the first time introduced to the formula-1 in 1980 by McLaren team. Since then the crashworthiness of the racing cars has improved beyond all

recognition. They used the carbon fiber composite to manufacture the body, which is low weight, high rigidity and provided the high crash safety standards [13].

The lightweight composite materials are already finding the exciting break in the automotive field as a means to increase the fuel efficiency. The vehicle weight directly contributes about 75 percent of fuel consumption. The vehicle industry can anticipate an aggressive 6 to 8 percent reduction in fuel consumption with 10 percent decrease in vehicle weight. This reduces around 20 kilogram of carbon dioxide emission per kilogram reduction in weight over the vehicle's lifetime [5].

The report from the united states and Canada predicted that plastics and composites would be widely used applied to body panels, bumper systems, flexible components, trims, drive shaft and transport parts of cars. Also rotors manufactured using RTM (Resin Transfer Moldings) for air compressor or superchargers of cars have been used to substitute for metal rotors which are difficult to machine [4]. Composites have been used to substitute flexi spline materials in harmonic drives [7].

CHAPTER 3

C.A.E TOOLS

3.1 CATIA V5

The CATIA V5 is geometric modeling software developed by Dassault Systems. It is the leading commercial computer program used in product development solutions for wide variety of industries, such as aerospace, automotive, electrical, electronics etc. which provides greater flexibility in modeling of the irregular contours.

CATIA V5 is the only solution capable addressing the complete product development process, from product concept specifications through product-in-service, in a fully integrated an associative manner. It facilitates the true collaborative engineering across the multi-disciplinary extended enterprise, including style from design, mechanical design and equipment and systems engineering, managing digital mock-up, machining, analysis, and simulation.

3.2 MSC Patran

MSC.Patran is a finite element modeler used to perform a variety of CAD/CAE tasks including modeling, meshing, and post processing for FEM solvers LSDYNA, NASTRAN, ABAQUS Etc. MSC Patran can be directly used to access the geometric models from leading design software's like CATIA, Pro-E etc. With use of many highly advanced tools presented in MSC.Patran helps to overcome the FEM challenges, including many topological irregularities multi body contacts and others.

Multi disciplinary analysis can be possible by using the open integrated CAE environment provided in MSC.Patran. This feature can be used to simulate manufacturing process and behavior of the product in early stages of design-to-manufacture process. This

has the ability to import geometry from any CAD system and various data exchange standards.

MSC.Patran provided with rich set of tools made it possible to achieve a required mesh quality with the different meshing techniques starting from completely automatic solid meshing to thorough node and element creation and editing. It also provided with different types of loads and constraints, which can be applied to either geometric model or to analysis model. The various visualization tools helps to find much critical information, including maximum and minimum values, contour plots which shows trends and correlations. Imaging features such as graphics shading, multiple light sources, local view manipulation and many other sophisticated visualization tools help to speed and improve results evaluation. It is also possible export result images and animation videos in many standard forms which help to present in reports.

3.3 LS-DYNA

LS-DYNA is a general purpose transient dynamic finite element program capable of simulating complex real world problems. It is optimized for shared and distributed memory UNIX, Linux, and Windows based, platforms. It is an explicit 3-D finite element program for analyzing the large deformation dynamic response of the elastic and inelastic solids and structures. The program is extensively used by many top automobile, aerospace and research organizations. A wide range of material types and interfaces enable the efficient mathematical modeling of many engineering problems.

It contains more than one hundred and fifty material models including metallic, non metallic and composite models which enable to define any material in the real world. The contact capabilities such as contact between deformable bodies, between deformable and

rigid bodies provided in LS-DYNA can solve any contact problems which very useful in crash testing.

The main application areas of LS-DYNA are as follows:

- Crashworthiness simulations: automobiles, airplanes, trains, ships, etc
- Occupant safety analyses: LS-DYNA integrated with MADYMO is used for dummy interaction with airbag, seat belts, foam padding, etc
- To simulate Bird strike to airplanes.
- Analysis and optimization of Metal forming process.
- Biomedical applications and many more.

LS-DYNA computes on leading UNIX machines, supercomputers mad Massively Parallel Processing (MPP) machines. Computer configuration depends on processing time and problem size. Super computers and MPP takes the advantage of multiple processes when the code is highly efficient. .

3.4 EASI CRASH DYNA (ECD)

EASI CRASH DYNA is the first fully integrated simulation environment specially designed for crash engineering requiring large manipulation capability. It can directly read files in IGES, NASTRAN, PAM-CRASH, MADYMA and LSDYNA data. ECD has unique features, which enable the crash simulation more realistic and more accurate. These are

Pre-Processing Features

- Fully automatic meshing and automatic weld creation
- Rapid graphical assembly of system models
- FE-Dummy and Rigid body dummy structuring, positioning and orientation

- Material database access and manipulation
- Graphical creation, modification and deletion of contacts, materials, constraints and I/O controls
- Automatic detection and correction of initial penetration
- Replacing the component from one model to another model

Post-Processing Features

- Highly optimized loading and animation of DYNA results for design
- Superposition of results for design
- User friendly and complete plotting for processing simulation and test data comparisons
- Quick access to stress energies and displacements without reloading the file
- Dynamic inclusion/exclusion of parts during animation and visualization
- Import and super-imposition of test results with simulation results
- Synchronization between animation and plots, between simulation result file and test result file

EASI-Plot Features

- User friendly complete plotting tool for processing simulation and test data
- Easy access to engineering functions
- Plot file re-generation using template and session file

CHAPTER 4

MODELING AND ANALYSIS OF THE IMPACT BEAM

The Finite Element Method (FEM) is used for the computational analysis of the behavior of new side door impact beam under impact loading with the aim to compare the capability of the impact energy absorption in relation to a current steel impact beam. The different fiber orientation of the composite beam are analyzed in order to find the most suitable sequence in terms of strength, stiffness, absorbed energy and weight

4.1 Design of the Side Door Impact Beam

The strength of the beam depends on the section modulus. Section modulus (Z) is defined by

$$Z = I/Ymax$$

I=Moment of Inertia

Ymax=distance from the Neutral axis

The common sections used for side impact beam are circular tubes, C sections, and rectangular tubes. In all these sections resistance to the deformation is increased by increase in the thickness.

The new beam is designed in accordance to fit the existing door. The new beam contains the double S curved side wings which offer additional strengthening, which cause the deflection to decrease. Some part of the beam is under tension and some part of the beam under compression, so the spring back effect is more in such a type of cross sections. The largest proportion of the absorbed energy, taken upon by side wings is in plastic region of the material deformation. It is expected that the side wings will curve inward under the

applied load. Smooth passage from one cross section to the other ensures that high stress concentration is avoided [2].

The beam is of length 947 mm. The strengthening region, where highest deflection and stress are expected, is 547 mm long and was chosen regarding to the position of the applied load. The beam cross section is shaped like double S. It is 55 mm wide in narrowest section and 105 mm wide in widest section. The thickness of the three dimensional is 2.3 mm for steel and 3.9 mm for carbon fiber composite and is constant throughout the whole structure. The mass of the total beam for steel is 2.64 Kg and for composite is 0.90 Kg.

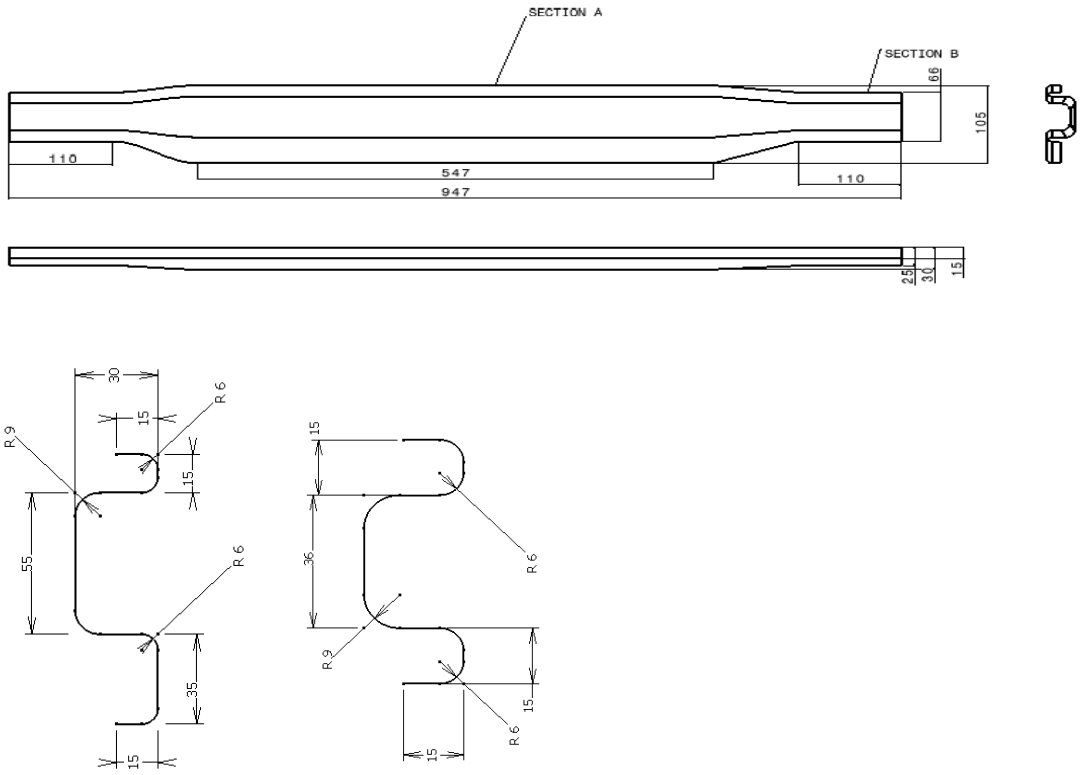

Section A Section B

Figure 7: Dimensions of Side Impact Beam

4.2 Comparison of Current Beam with New Beam

- Current beam has C cross section and the new beam has double S cross section.
- Current beam has uniform width throughout but the new beam has more strengthening in the middle.
- Current beam has cornered edges, so there will be discontinuity in force distribution. The new beam has round edges, so smooth force distribution.

4.3 Material Description

The carbon fiber composites are light weight material because of its low density. The mechanical properties of the carbon fiber are very much suitable as they have high impact energy absorption before fail and also they have high strength requirements. The mechanical properties of the carbon fiber composites can be changed according to the requirement by changing orientation of the fiber in the loading direction, layer stacking and by changing the volume fraction of the fiber and the matrix.

Carbon fiber composite can sustain the same load as of steel even with the 40 percent of the steel weight. The carbon fiber composites have very high specific strength and specific stiffness when compared to steel.

Table 1: Material Properties for Carbon Fiber Laminate

Mass Density	**1.58 g/cc**
Longitudinal Modulus E1	**142GPa**
Transverse Modulus E2	**10.3GPa**
Inplane Shear Modulus G12	**7.2GPa**
Poisson's Ratio	**0.27**
Longitudinal Tensile Strength F1t	**1830Mpa**
Transverse Tensile strength F2t	**57MPa**
Inplane shear Strength F6	**71MPa**
Longitudinal Compressive Strength F1c	**1096MPa**
Transverse Compressive Strength F2c	**228Mpa**

Table 2: Material Property for Steel

Mass Density	**7.8 g/cc**
Young's Modulus	**200 GPa**
Poison's Ratio	**0.3**
Yield Stress	**0.215 GPa**

4.4 Beam Modeling

The geometric modeling of the side impact beam is done by using CATIA V5 and mesh, boundary conditions, material properties and section properties are defined using MSC.Patran. The beam is uniformly meshed with 10 mm element size. The beam is meshed with shell elements. The ends of the beam are constrained in all the directions both in

translational and rotational. Belytschko Tsay element formation is used, because it gives better results with bending stress.

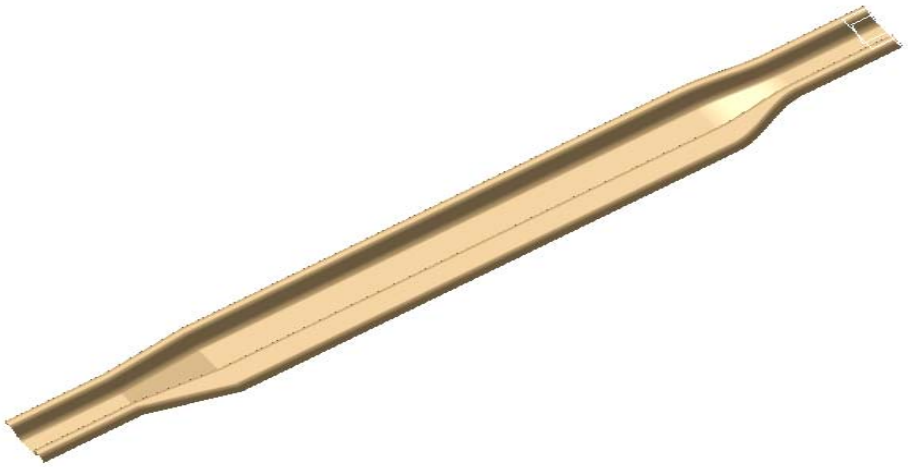

Figure 8: Side Impact Beam

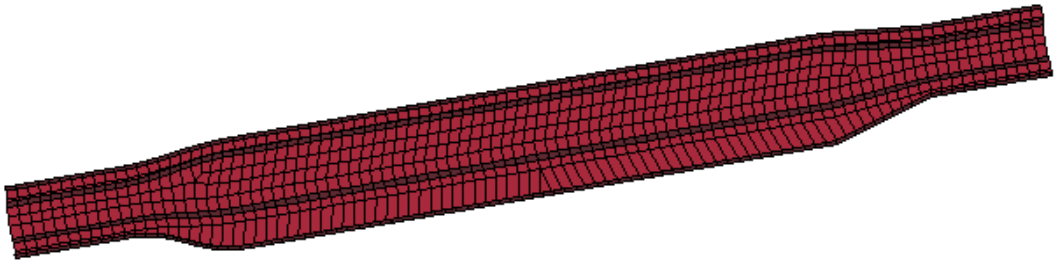

Figure 9: Side Impact Beam with Mesh

Table 3: Beam Model Summery

Element Length	10mm
Number of Nodes	3062
Number of Elements	1684

4.5 Modeling of Impact Body

The solid cylinder is considered as impact body. The impact body is considered an analytically rigid body with mechanical properties of the steel. The diameter of the impact body is 200mm and the height is of 150 mm. The impact body is coarse meshed with the element size of 20mm, since the number of elements does not influence the solution. Weight of the impactor is 20 kg.

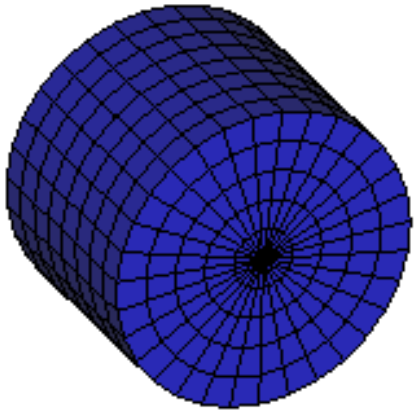

Figure 10: Impactor

Table 4: Impactor Model Summary

Element Size	20mm
Number of Nodes	1449
Number of elements	1280

4.6 Current Impact Beam

The current Impact beam is C section with the length 947 mm long and 105 mm wide with a uniform thickness of 2.3 mm. The weight of the beam is 2.44 Kg. Steel is the material used.

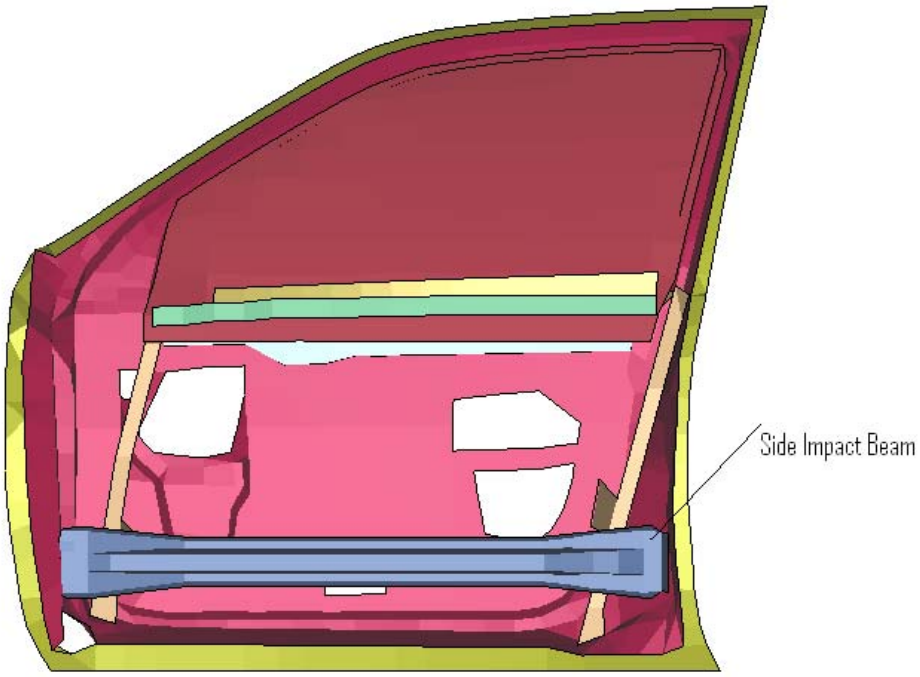

Figure 11: Current Side Impact Beam with Door

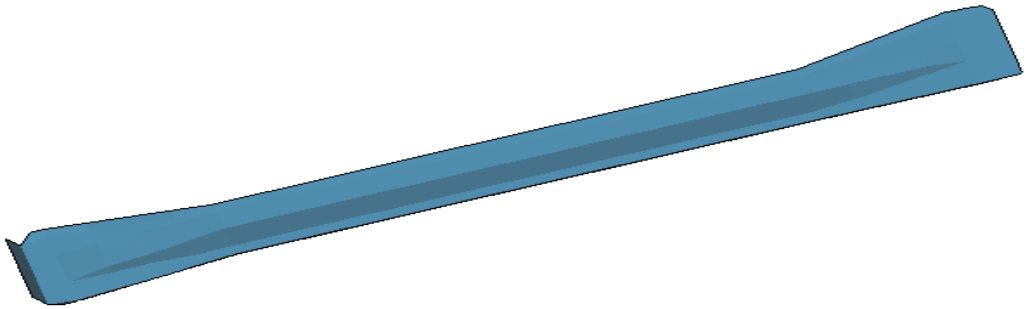

Figure 12: Current Side Impact Beam

4.7 Optimization of the Composite Impact Beam

The ply orientation and the thickness of the composite beam are found out by simulating the composite beam for different orientation and different thickness. The force displacement curve is plotted to find the total energy absorption.

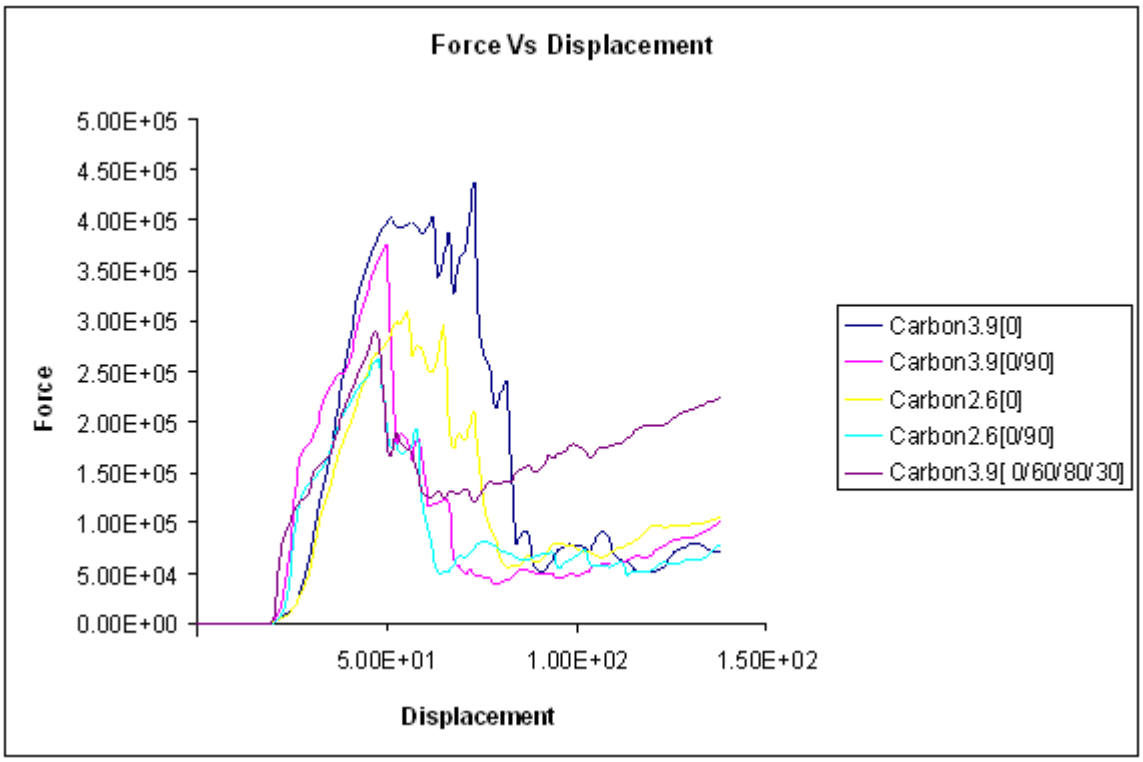

Figure 13: Force Displacement Curve for Different Fiber Orientation and Thickness

Table 5: Summary of Composite Beam under Impact Loading

Orientation	No of Plies	Thickness of ply(mm)	Peak Load(KN)	Total Energy(KN/mm2)
0/90	13	0.3	4.5E+02	1.72E+04
0/90	13	0.2	3.0E+02	0.94E+04
0/90/±45	13	0.3	3.5E+02	1.52E+04
0/30/±60/±80	13	0.3	2.7E+02	1.64E+04
0/90/±45	13	0.2	2.5E+02	1.12E+04

MAT_ENHANCED_COMPOSITE_DAMAGE is the LS-DYNA material card used to define the composite material property of the composite material. This card is used to define orthotropic property of composite material e.g. shell structure of unidirectional composite layers. This material card has special measures to failure under compression. This card can be used to only shell elements.

Different combination of 0, 30, 45, 60, 80, and 90 are tested with the thickness of 2.6 and 3.9 mm. The total number of plies in the beam is 13 with thick ness of 0.2 to 0.3 mm. Total energy absorption and Peak load are the two factors considered in selecting the composite material orientation and thickness of the beam. From the Figure 4.7 and table 4.5 we can see that the beam with thickness 13 mm and orientation 0/30/±60/±80 gives the better result, which is selected for further studies.

4.8 Comparison of Beam at Different Impact Angles

The composite beam with the orientation 0/30/±60/±80 is tested for different impact angles in order to justify the difference in the orientation angle of fiber in real scenario.

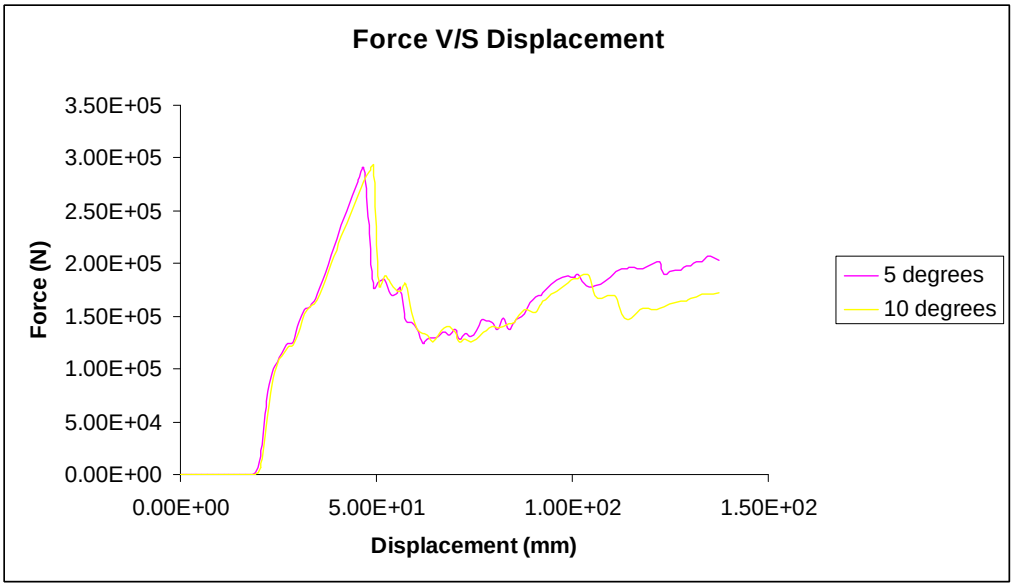

Figure 14: Force Displacement Curve for Different Impact Angles

Table 6: Energy Absorption of Composite Beam for Different Impact Angles

Vertical offset angle(degrees)	Peak Load (KN)	Total Energy (KN/mm2)
0	2.7E+02	1.64E+04
5	2.7E+02	1.69E+04
10	2.7E+02	1.68E+04

From the figure 4.8 and table 4.6 we can see that there is no much change in the peak value of force and total energy absorption. This shows that the there is no much difference in the results due to small changes in the orientation angle in the fibers.

4.9 Weight Comparison

Total weight of the new composite is 65 percent less when compared to the total weight of the new steel beams and absorb more deformational energy. Thickness of the composite beam is of 3.9 mm in order to maintain the same stiffness and energy absorption.

Table 7: Side Impact Beam Weight

Weight of current Beam	2.44 Kg
New Beam with Steel	2.64 Kg
New Beam with Composite	0.90 Kg

4.10 Comparative Analysis of Impact Beam

The comparative analysis of the Impact beam is carried out by finding the total energy absorption of the beam under impact loading. The Beam is fully constrained at the ends. The impactor is considered as a rigid body with mass 20 kg and diameter of 200 mm

cylinder. The initial height of the impactor is 20 mm from the beam. The initial velocity of 33 mph is given to the impacter and hit the beam at the center.

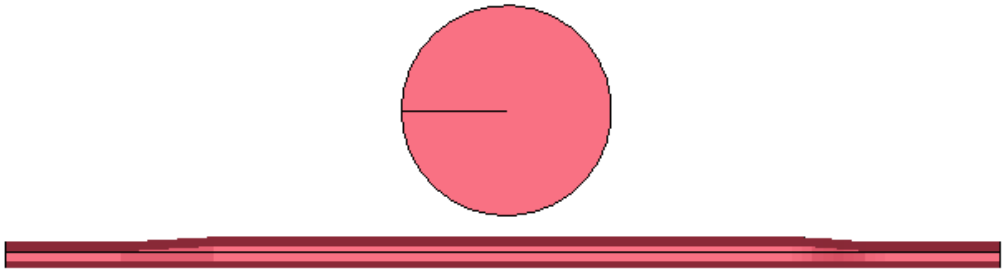

Figure 15: New Side Impact Beam before Impact

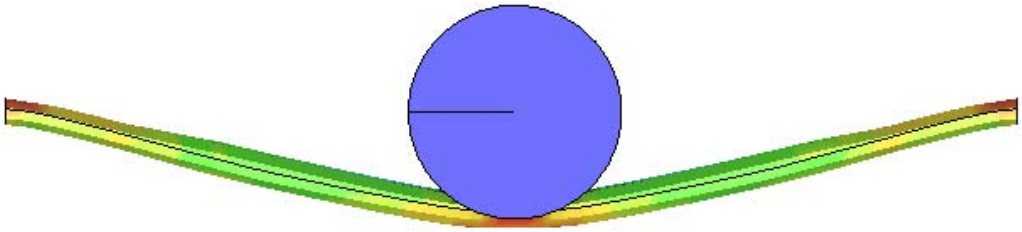

Figure 16: New Side Impact Beam after Impact

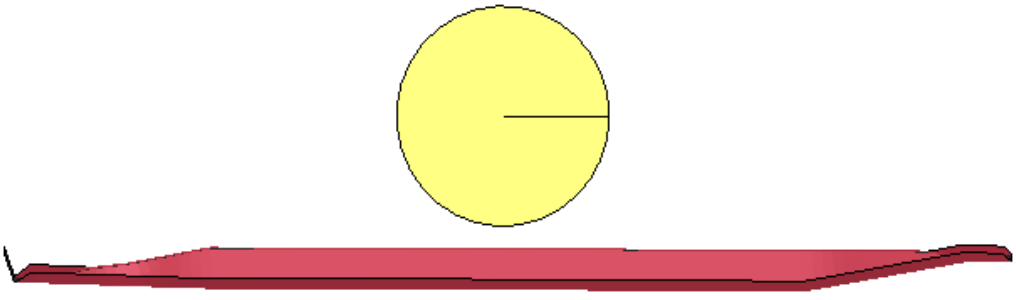

Figure 17: Current Side Impact Beam before Impact

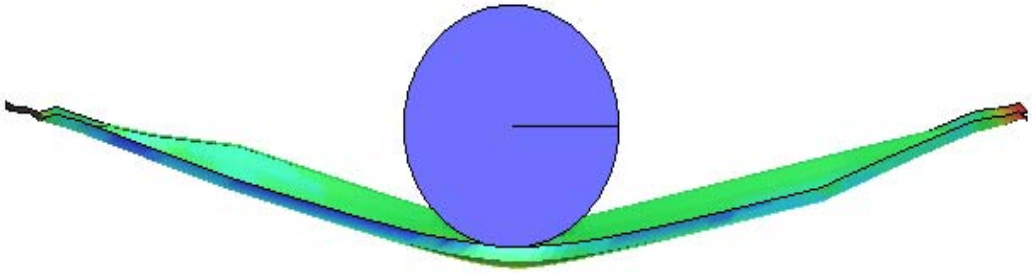

Figure 18: Current Side Impact Beam after Impact

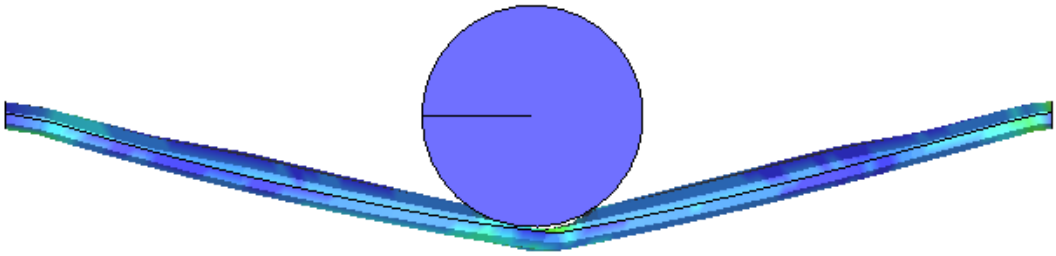

Figure 19: New Side Impact Composite Beam after Impact

4.11 Energy Absorption

4.11.1 Comparison between new beam with the current beam

The total energy absorption of the Impact Beam is found out by finding the area under the force displacement curve. The total energy absorption of the new Impact beam and old Impact beam is compared.

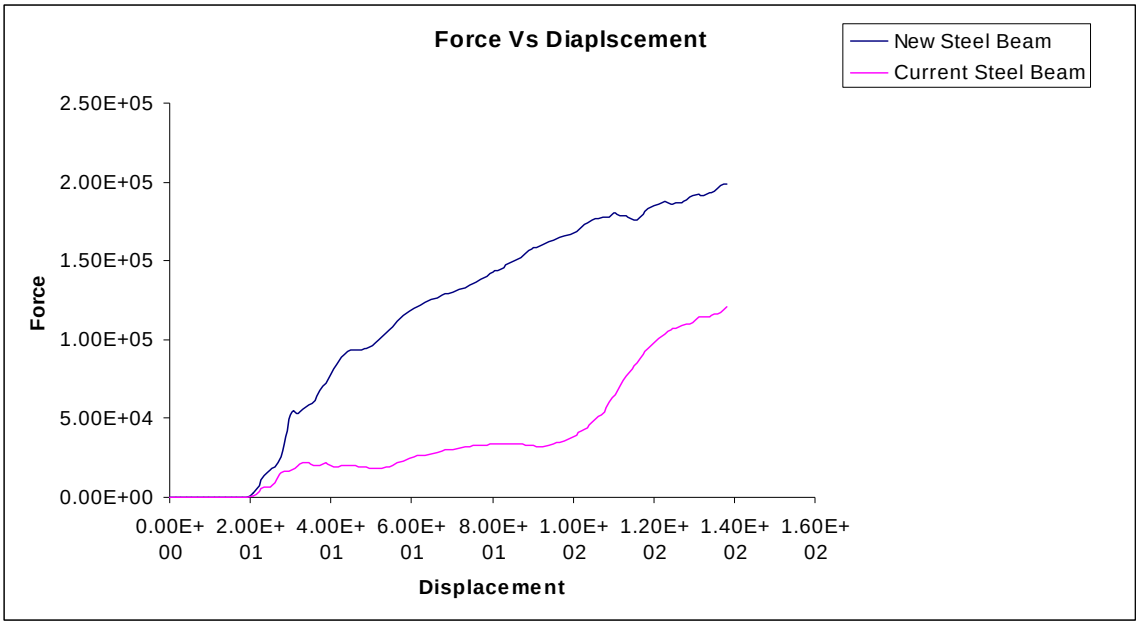

Figure 20: Force Displacement curves for New and Current Beam

From the figure 4.14 and the table 4.8 shows that the total energy absorption of the new beam is about 3 times more than that of current beam. This indicates that the new beam absorbs more energy and deforms less when compared to the current beam. This is because the new beam has reinforced more where the impact is common and more spring back effect due to the double s shape cross section of the beam.

4.11.2 Composite beam with steel beam

The energy absorption of the new beam with steel property is compared with the carbon fiber composite beam. The orientation and the thickness of the composite beam are found out by running the different simulation in order to get the best orientation and optimum thickness of the beam. The thickness of the steel beam is same as the thickness of the current beam.

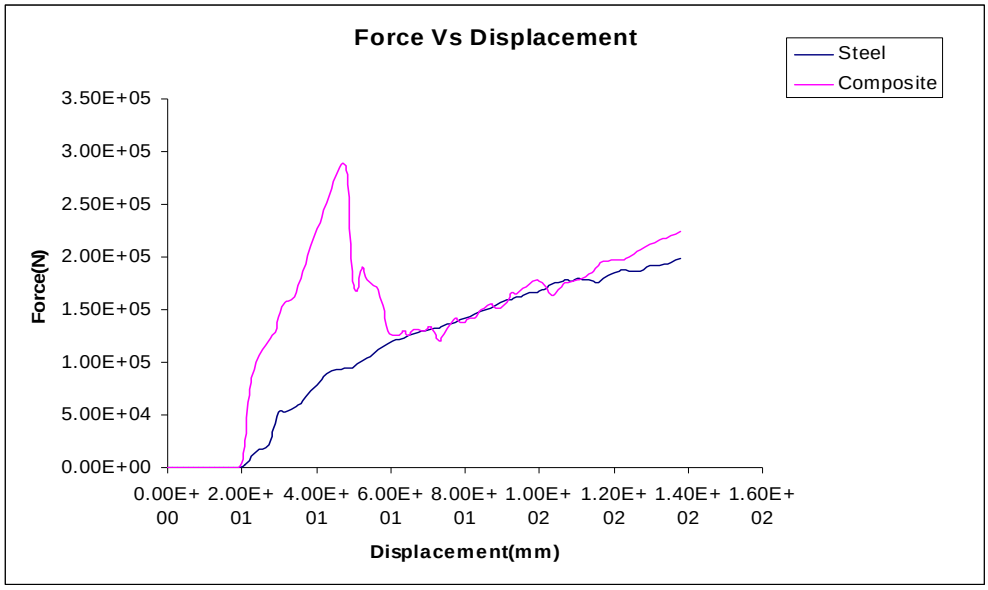

Figure 21: Force Displacement Curve for Steel and Composite

Figure 4.15 shows that initially there is a rapid increase of force in composite beam, this is because of the high stiffness of the carbon fiber composite beam. After initial increase force the beam starts absorbing energy by crushing of the fibers.

Table 4.8 shows that the total energy absorption of the composite is slightly more and weight of the composite beam is less by 65 percent.

4.12 Total Energy Absorption

From the table 4.8 we can see that the total energy absorption of new beam with steel is about three times more than the total energy absorption of the current beam, and the composite beam with new design absorbs even more energy than the new beam with steel.

Table 8: Total Energy Absorption of Side Impact Beam

Current Beam	5.26E+03 KN
New Beam With Steel	1.52E+04KN
New Beam With Composite	1.64E+04KN

CHAPTER 5

SIDE IMPACT MODELING

Federal Motor Vehicle Safety Standard (FMVSS) 214 is the regulation for Side Impact Protection developed by National Highway Traffic Safety Administration (NHTSA). NHTSA also developed a mathematical model for simulation of side impacts; the mathematical model simulates the responses of the MDB, the struck car. The Impact energy from the MDB is transferred to the struck vehicle through the pillars and the door sections.

5.1 Finite Element Model of Ford Taurus

The finite element model of the vehicle is generally developed by reverse engineering process that virtually generates vehicles. These models are accurate enough to analyze different crash test configurations and to predict the vehicle and occupant behaviors in various crash scenarios. Such a design leads to minimize the time and the cost of the testing process and helps in making effective safety decisions.

The general procedures the researchers use to generate FEA vehicle model are

- Apply tape over the entire vehicle to get an accurate representation of the geometries.
- Digitize every component using a seven-degree-of-freedom coordinate measuring machine
- Disassemble all the vehicle components.
- Collect the mass and the material thickness data for vehicle and individual parts.
- Identify all the parts and connections.
- Conduct center-of-gravity calculations.

- Execute material property tests for component strength.
- Create a computerized “mesh” grid of the vehicle using advanced computer codes.
- Reconnect all parts accurately, including spot welds, rigid body constraints, joints, springs and dampers.

Table 9: Model Summary of Ford Taurus Car

Number of Parts	134
Number of Nodes	26797
Number of Quad Elements	23124
Number of Tria Elements	4750
Number of Hexa Elements	338
Number of Penta Elements	10
Number of Discrete Elements	2

The Ford Taurus model which is used in this thesis is a four door sedan with 5 meters length and 2.76 meter wheelbase. It is developed by National Crash Analysis Center. Figure 5.1 shows the finite element model of the Ford Taurus car. It has 134 parts which represent different vehicle parts. The parts are joined by rigid body constrained options and spot weld. The contacts between different parts are modeled as single surface sliding interface (AUTOMATIC_SINGLE_SURFACE).

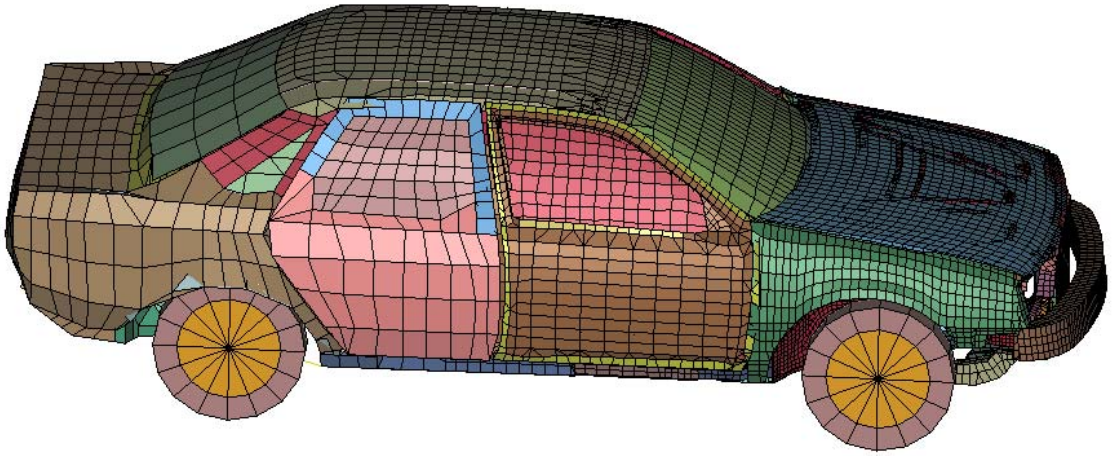

Figure 22: Finite Element Model of Ford Taurus

Table 10: Material Properties of Ford Taurus Car

Mass Density	7890 Kg/m3
Young's Modulus	210E+09 N/mm2
Yield Stress	270E+09 N/mm2
Poisson Ratio	0.3

5.2 Impactor Modeling

Mass and geometry of the MDB defined in FMVSS 214 (Side Impact) represents the general U.S vehicles. The impact angle represents the most common side impact. The relative speed and direction of the MDB and the target vehicle is considered the threshold for serious injury in actual crashes.

The MDB face assembly includes a bumper constructed of honeycomb 1690+/-103 kPa sandwiched between 3.2 mm thick aluminum plates. The bumper is a flexion member and develops flexion strength based on the material properties of these front and back plates.

The moving deformable barrier (MDB) is used as the impactor. The impact face of the barrier is made from aluminum honeycomb structure. The bottom edge distance of MDB from ground is 279 mm. The extending part of the barrier, which represents a bumper, is 330 mm from ground. The total mass of the MDB is 1367 kg. For defining material model in LS-DYNA for honeycomb structure of the barrier face, MAT_HONEYCOMB card has been defined.

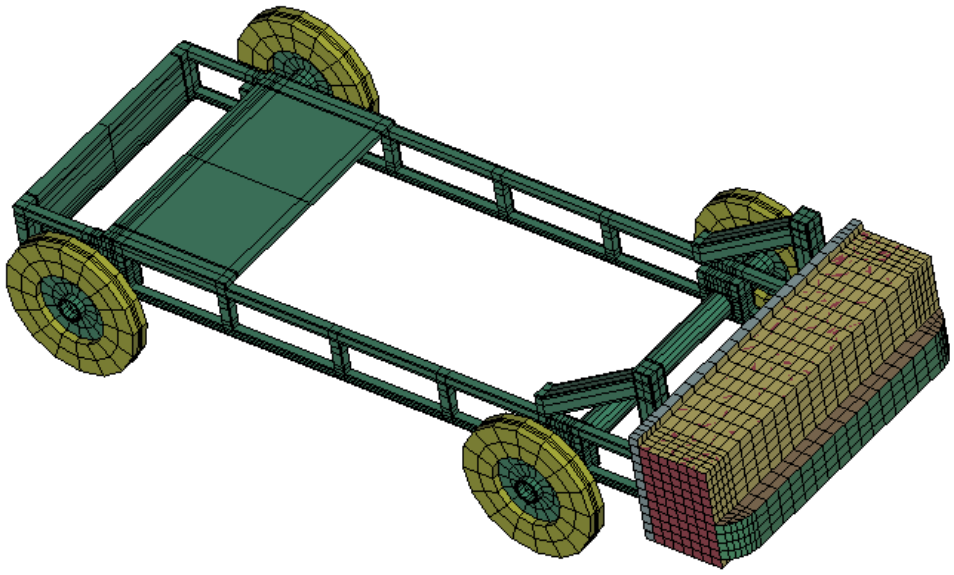

Figure 23: Finite Element Model of Moving Deformable Barrier

Table 11: Model Summary of Moving Deformable Barrier

Number of Parts	8
Number of Nodes	11033
Number of Quad Elements	718
Number of Hexa Elements	7324

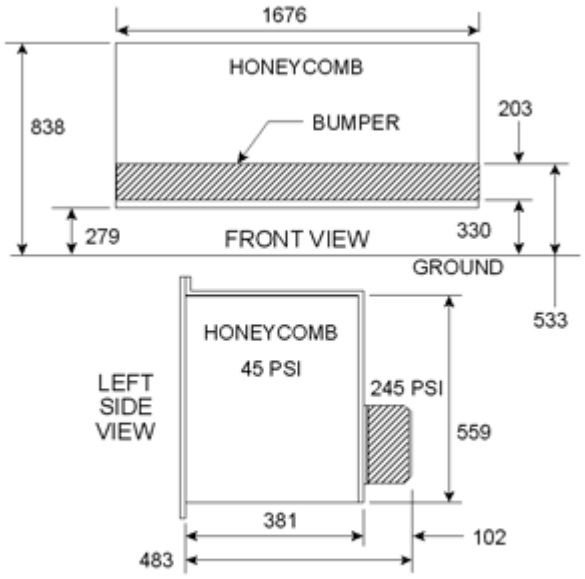

Figure 24: Moving Deformable Barrier Face [1]

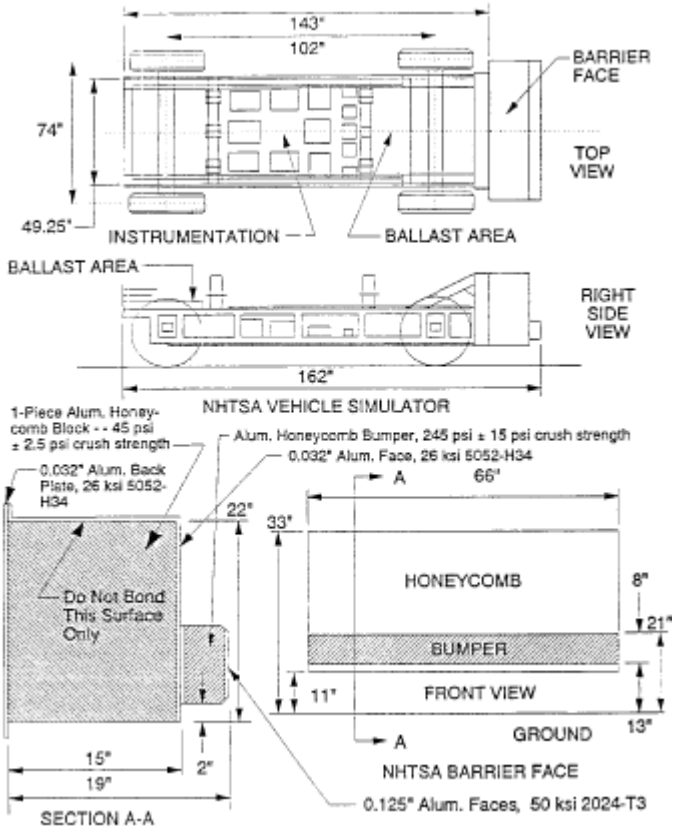

Figure 25: Dimensions of Moving Deformable Barrier [1]

CHAPTER 6

RESULTS AND DISCUSSION

6.1 FMVSS 214 Test Configuration

The test Vehicle is stationary. The line of action of the Moving Deformable Barrier makes an angle of 63 degrees with the test vehicles centerline. The longitudinal centerline of the moving deformable barrier is perpendicular to the longitudinal centerline of the test vehicle when the barrier strikes the test vehicle. In a test in which the test vehicle is to be struck on its left side: All wheels of the moving deformable barrier are positioned angle of 27 degrees to right of the centerline of the moving deformable barrier.

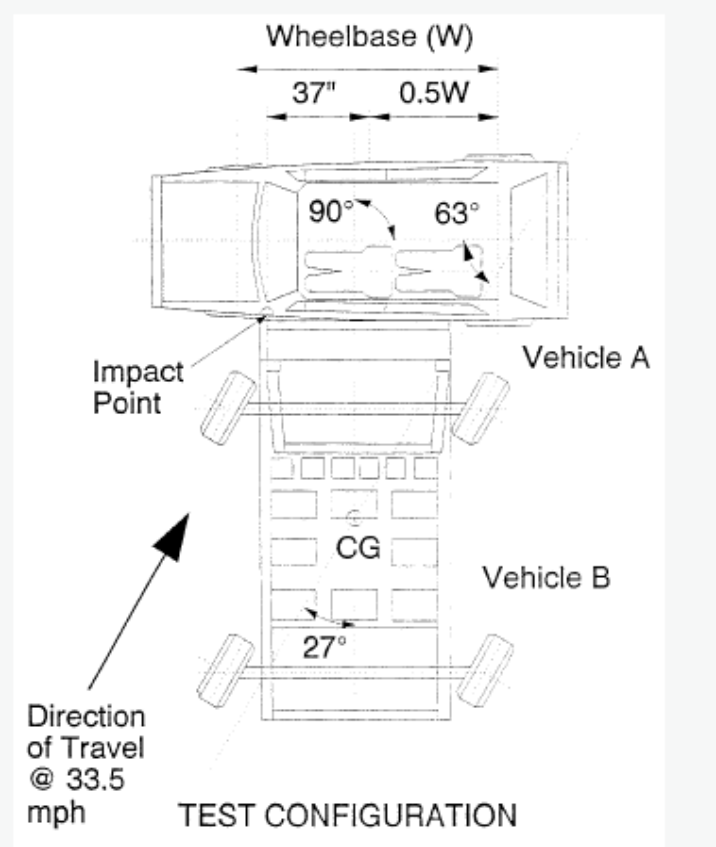

Figure 26: FMVSS 214 Test Configuration [1]

6.1.1 Simulation results with current side impact beam

The Ford Taurus car with current impact beam is impacted by the Moving Deformable Barrier according to the FMVSS 214. Figure 5.2 shows the finite element model of the side impact after crash. According to FMVSS 214, the moving deformable barrier hits the driver side of the stationary car at an angle of 27 degrees with the longitudinal axis of the barrier at an angle 33.5 mph.

The full Side Impact model is carried out in LS-DYNA for 0.2 seconds. The accelerometers are placed at eight locations in the vehicle. The contacts are defined by geometric interface. The distance between the vehicle and the barrier is kept to be minimal in order to minimize the simulation time.

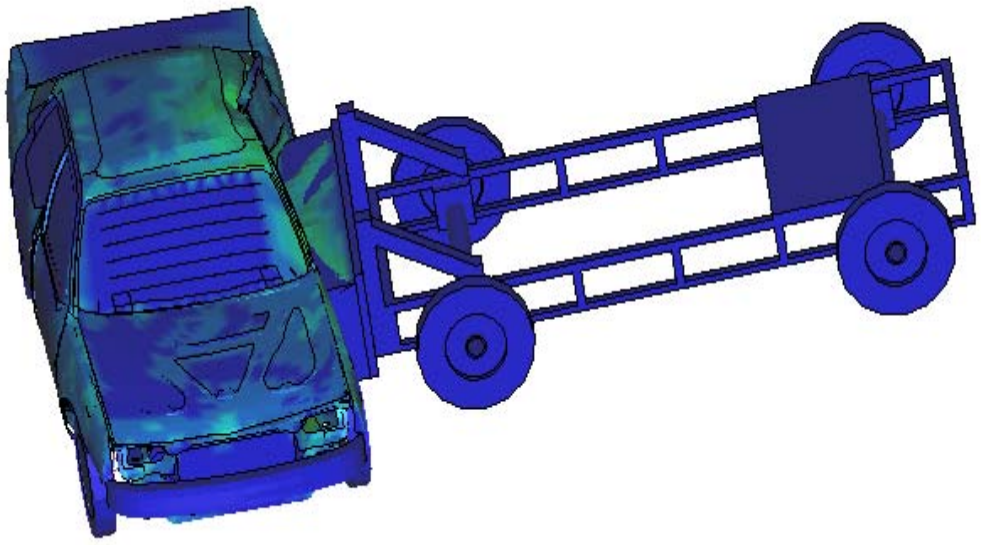

Figure 27: Side Impact Model of Ford Taurus car

There is considerable deformation of side door structure with the side impact beam can be seen from the Figure 6.3.

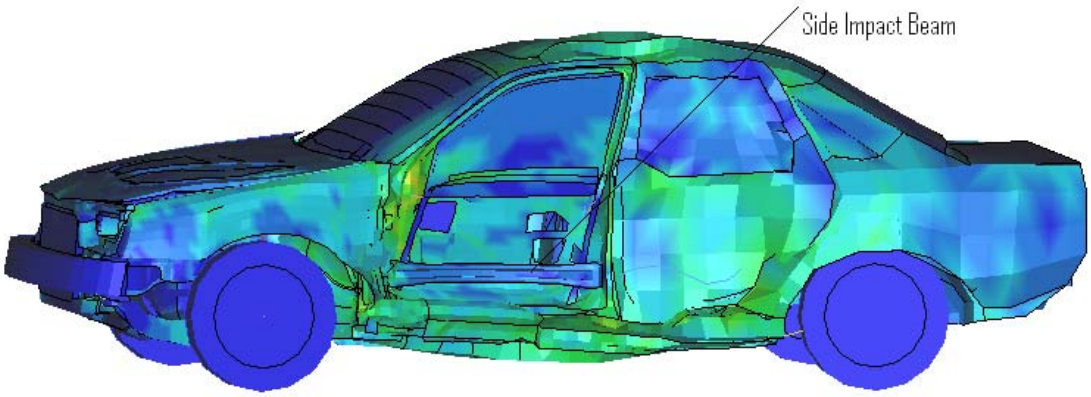

Figure 28: Car Model after Impact

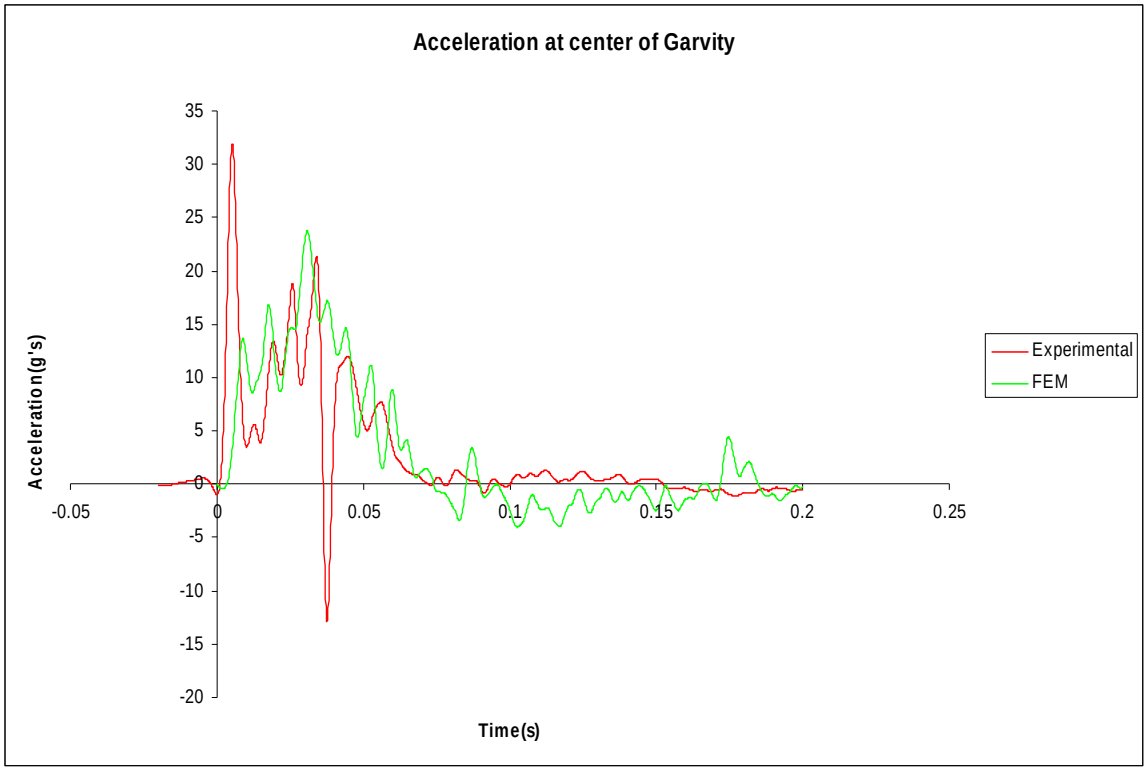

Figure 29: Acceleration at Center of Gravity of the Car

The acceleration at the Center of Gravity for both experimental and Finite Element Model are shown in the figure 6.4. Mathematical model of the Ford Taurus car is specially designed for frontal crash, therefore the large variation in peak values for both the models. Also the

placement of the accelerometer in both the cases may cause the large variation in the out put value. The patterns of the Finite Element curve are almost similar to the pattern of the experimental curve.

6.1.2 Simulation results with new steel side impact beam

The new impacts beam is merged to the car model by using EASI-CRASH DYNA. The beam is fixed to the side door frames and nodes in the edge of the beam are fixed with the neighboring nodes in the side door frame, which constrains the relative motion of the nodes. The CONTRAINED_NODAL_RIGID_BODY is the LS-DYNA card used to constrain the beam to the door.

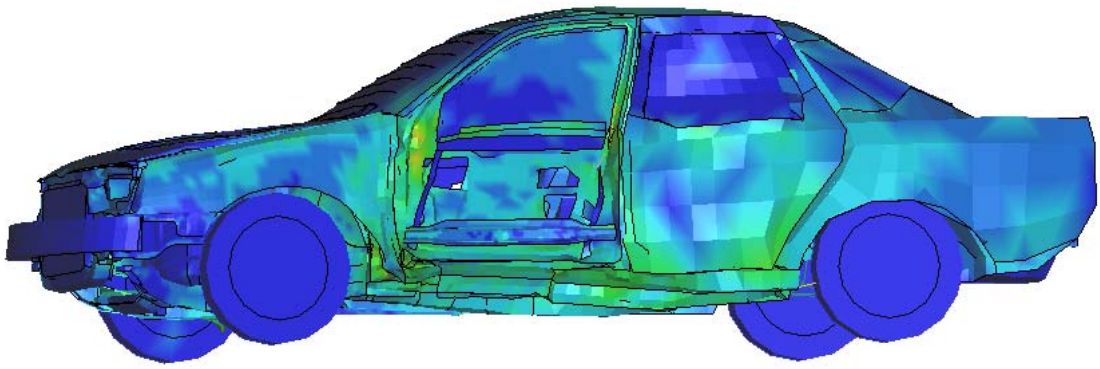

Figure 30: Car Model with New Impact Beam after Impact

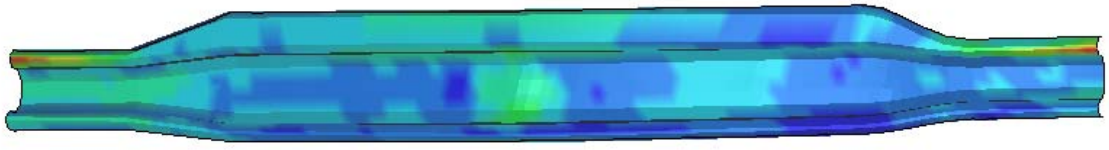

Figure 31: New Side Impact Beam after Impact

6.1.3 Comparison of current steel beam with new steel beam

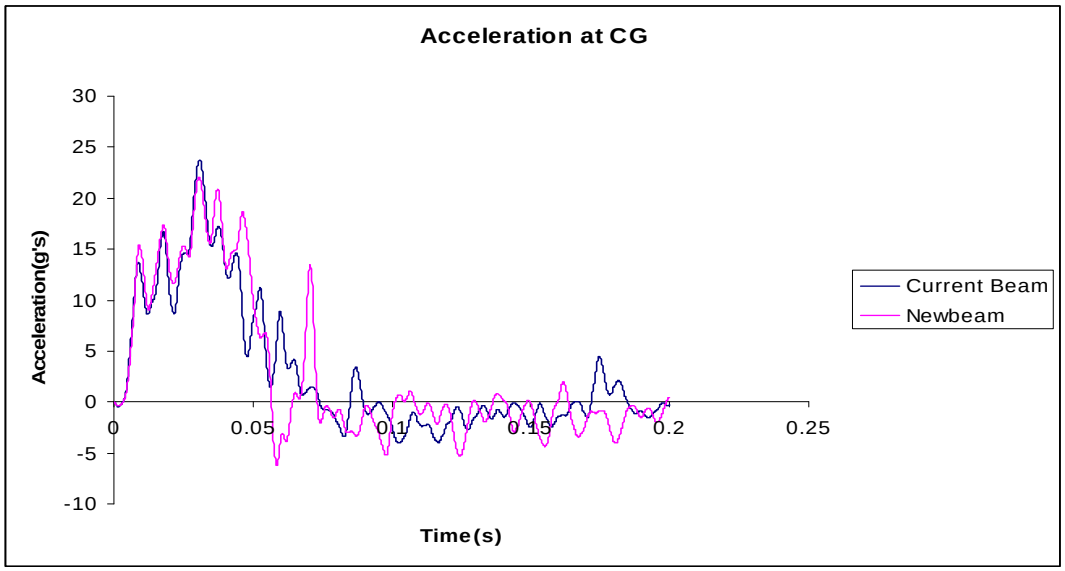

Figure 32: Acceleration at Center of Gravity

Figure 6.7 shows the comparison of the Acceleration at the Center of Gravity for the Ford Taurus car with the Current side impact beam and new impact beam. The mass of the side impact beam is almost 0.1 percent of the total mass of the car and velocity of impact is high so there is no much difference in both the curves, but the peak value with the new beam is less by 3 g's.

6.1.4 Intrusion of the beam

Intrusion of the beam is found out by subtracting the displacement of the node which is attached to the frame of the door where the beam is not deforming with the node at the center of the beam where the deformation is more.

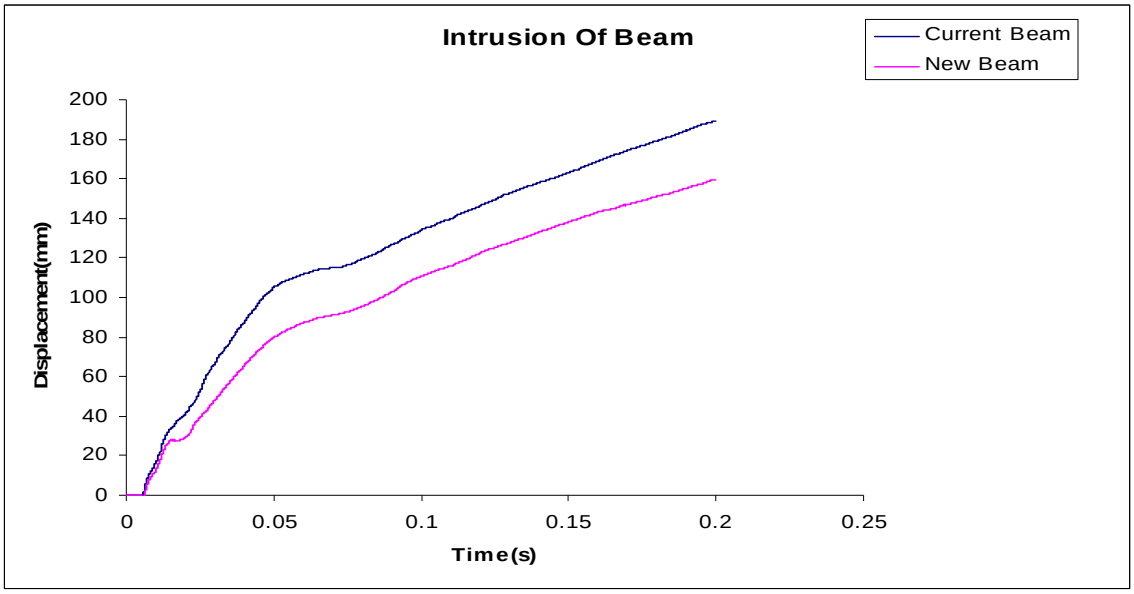

Figure 33: Intrusion of Beam with Steel

Figure 6.8 shows the comparison of intrusion in current steel beam with new steel beam. The intrusion in the new steel beam is less by 20 percent when compared to the current beam. From the figure we can see that the intrusion in new beam is less throughout the crash duration.

6.1.5 Acceleration of the impact beam

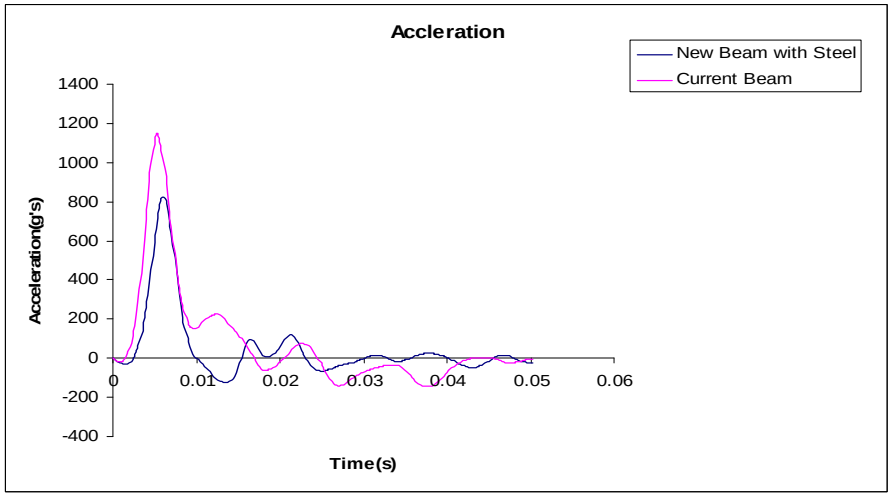

Figure 34: Acceleration of the Beam with Steel

Figure 6.9 shows the comparison of acceleration at the center node of the current and new side impact beam. From the figure we can see that the acceleration in the new side impact beam is less by about 33 percent g's when compared to the current impact beam. The mass of the beam is 0.1 percent of the total mass of the car and the impactor with 1367 kg is made to hit with velocity of 33.5 mph, so the beam experiences higher g's.

6.1.6 Comparison of new beam with steel and composite

Intrusion of the new beam with steel and composite is shown in the figure 6.10. From the graph we can see that the displacement of the composite beam is decreasing after initial increase, because of the spring back effect due to high stiffness of the composite beam.

From the below graph we can see that the intrusion in composite beam is about 25 percent less when compared to the steel beam.

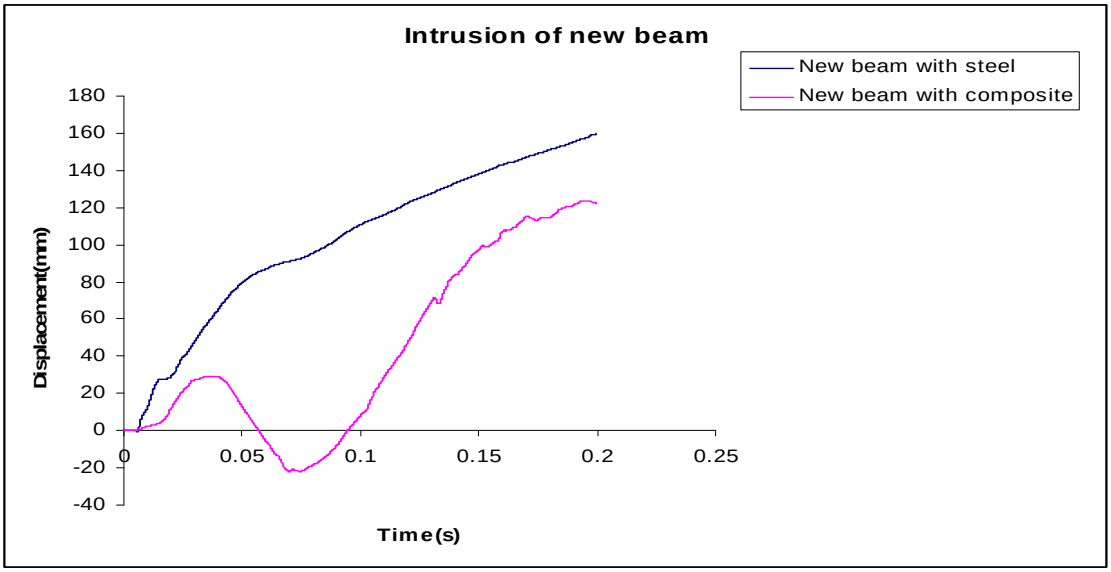

Figure 35: Intrusion of New Beam

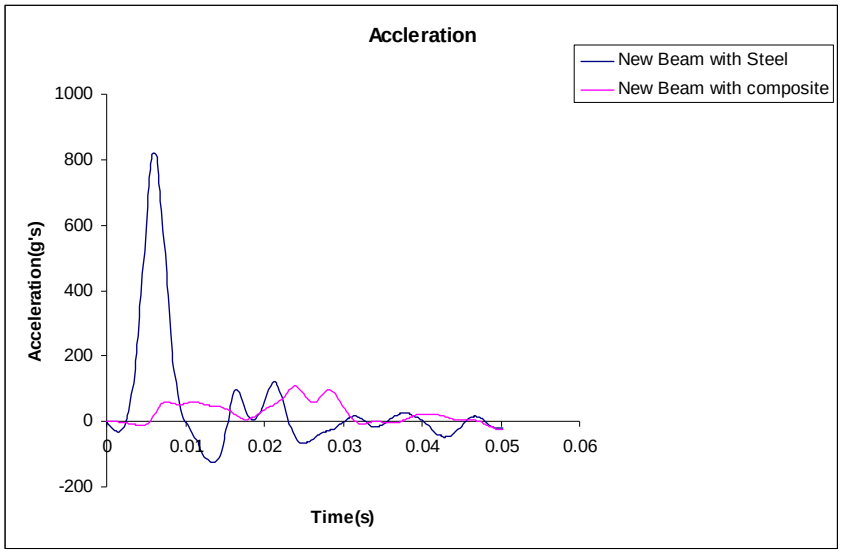

Figure 36: Acceleration of New Beam

Figure 6.11 shows the comparison of new steel beam with composite beam. The acceleration in the composite beam is about 70 percent less when compared to the acceleration in the steel beam.

6.2 Insurance Institute for Highway Safety (IIHS) Side Impact Test Configuration

The test vehicle aligned with the Moving Deformable Barrier (MDB) is shown in the Figure 6.12. In IIHS test procedure the Moving Deformable Barrier strikes the stationary Ford Taurus car with a velocity of 31 mph (51 kmph). In case of IIHS the wheels of the Moving Deformable Barrier (MDB) are aligned with the longitudinal axis of the barrier to allow for 90 degree impact.

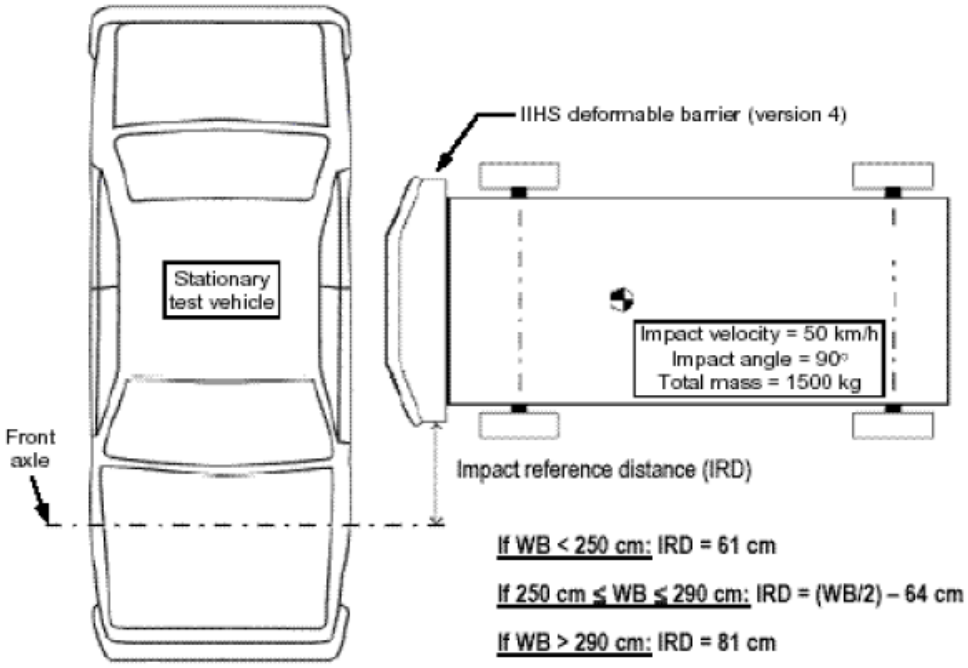

Figure 37: IIHS Side Impact Test Configuration [3]

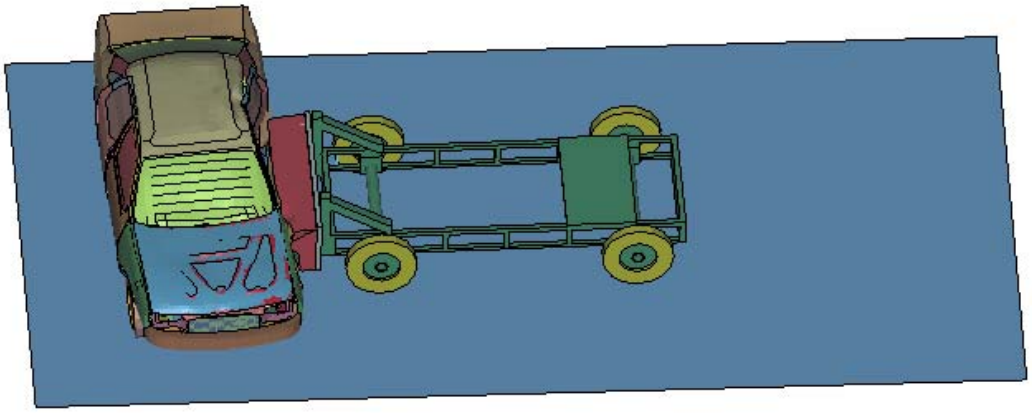

Figure 38: Side Impact Model for Ford Taurus Car

6.2.1 Comparison of current steel beam with new steel beam

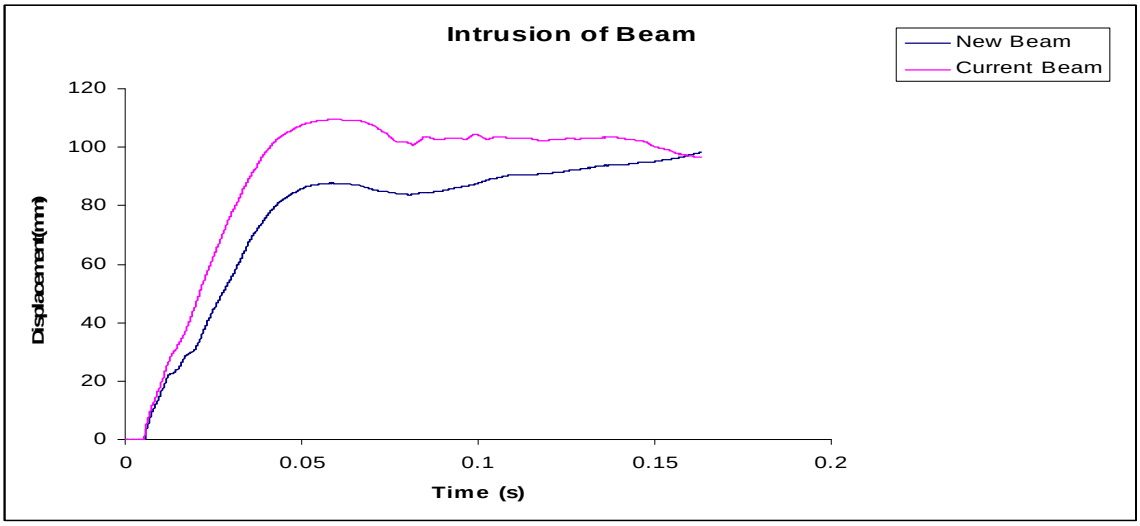

Figure 39: Intrusion of Steel Impact Beam

Figure 6.14 shows the comparison between the intrusions of current steel beam with new steel beam. From the figure we can see that the intrusion in new beam is 35 percent less when compared to the current beam at 0.05 seconds. Intrusion in the new beam is less throughout the crash duration.

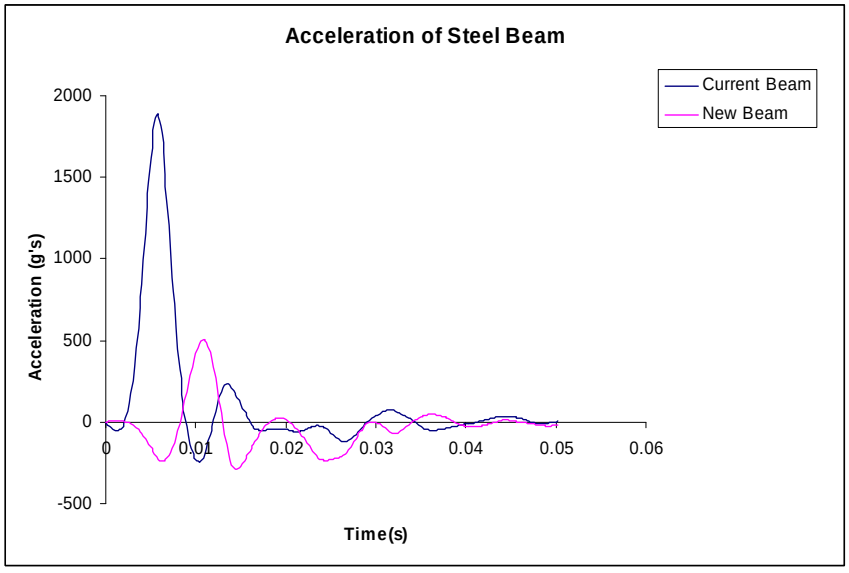

Figure 40: Acceleration of Steel Impact Beam

Figure 6.15 shows the comparison between acceleration in the current beam with steel beam. The acceleration in the new beam is about 74 percent less than the current beam.

6.2.2 Comparison of new steel beam with composite beam

Figures 6.16 shows the comparison between the new steel beam with the new composite beam. From the figure we can see that the intrusion in composite beam is about 40 percent less when compared to the steel beam.

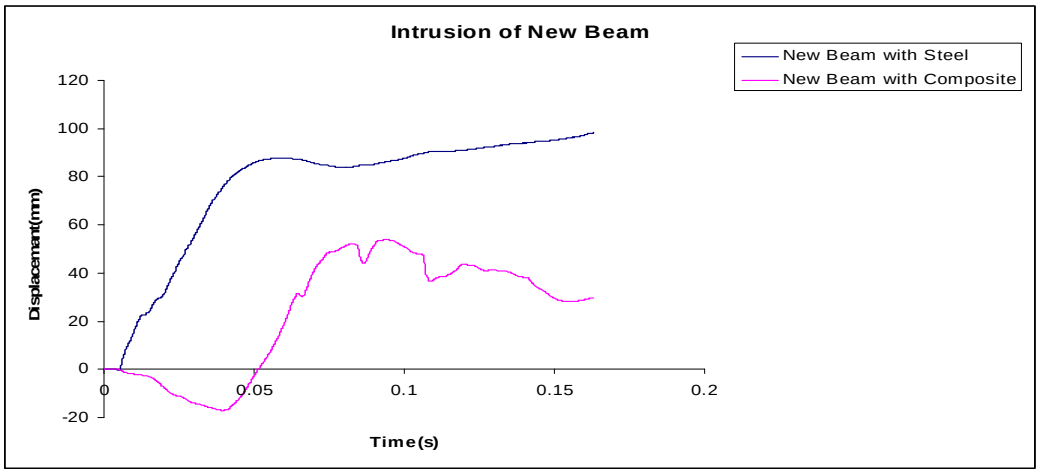

Figure 41: Intrusion of New Impact Beam

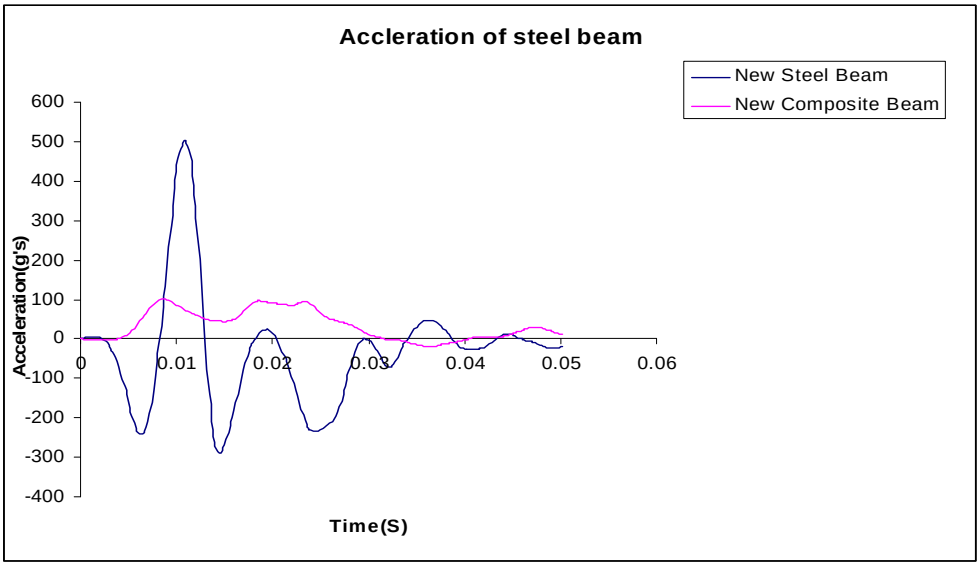

Figure 42: Acceleration of New Impact Beam

The figure 6.17 shows the comparison between acceleration of new steel beam with the new composite beam. From the figure we can see that the acceleration in the composite beam is about 78 percent less when compared to the acceleration of the new steel beam.

CHAPTER 7

CONCLUSIONS AND RECOMMENDATIONS

Total energy absorption of the current beam, new beam with steel and new beam with composite material is compared. Effectiveness of the above beams is compared by testing the beams according the FMVSS 214 and IIHS side impact protection test methods.

By implementing the new side impact beam the intrusion of the side door can be reduced, eventually reducing the occupant injuries.

By comparing the computational results of steel beam with the composite beam it can be concluded that

- There is considerable reduction in the weight of the beam.
- Composite beam can absorb more deformational energy than steel and more effective than steel even 65 percent reduction in weight.
- Composite beam is more effective for both FMVSS 214 and IIHS side impact protection standards.
- User can optimize the mechanical properties of the composite material by changing the fiber orientation and fiber matrix volume ratio.
- Composite materials are replaceable where high strength and high stiffness are required.

Although the composite beams fail by buckling during impact loading, by proper design, fiber orientation and fiber matrix combination buckling failure can be reduced.

The following are the future recommendations which can be addressed by using composite material with new design

- Experimental validation can be done before practical implementation of the composite beam in automobile industry.
- The effectiveness of the new beam with composite material can be verified by finding the occupant injury parameters using MADYMO.
- Effectiveness of the beam can be improved by using different cross sections.
- Manufacturing of the composite beam is still a costly process; it can be reduced by developing the simple manufacturing process.

REFERENCES

LIST OF REFERENCES

[1] Federal Motor Vehicle Safety Standards (FMVSS) No.214 “Side Impact Protection, 2005.

[2] Erzen S., Ren Z. and Anzel I, “Analysis of FRP Side-Door impact Beam,” 2002.

[3] IIHS, Crashworthiness Evaluation Side Impact Crash Test Protocol (version III) April 2004.

[4] Cheon, S.S., Dai, G.L., and Kwang, S.J., “Composite side-door impact beams for passenger cars,” Composite Structures, Vol 38, No 1-4 pp. 229-239, 1997.

[5] Kanianthra, J.N., Rains, G.C., and Trella, T.J., “Strategies for passenger car design to improve Occupant protection in real world side crashes,” 1993.

[6] www.azom.com/news, “Fuel Efficiency Stimulates Use of Lightweight Materials in Automobile Industry,” (Cited 2005).

[7] Patberg, L., Philips, M., Dittmann, R., “Application of Fiber-Reinforced Composites in the Car Side Structures,” Society of Automotive Engineers, Inc, 1998.

[8] Farely, G.L., “Energy Absorption of Composite Materials,” Journal of composite Materials, Vol. 17, pp. 267-279, 1983.

[9] Thornton, P.H., and Jeryan, R.A., “Crash Energy Management in Composite Automotive Structures,” International Journal of Impact Engineering, Vol 7, No 2, pp 167-180, 1988.

[10] Schmueser, D. and Wickliffe, L.E., “Impact Energy Absorption of Continuous Fiber Composite Tubes,” Journal of Engineering Materials and Technology, Vol 109, pp.72-77, 1987.

[11] Ramakrishna, S. and Hamada H., “Energy Absorption Characteristics of Crash worthy Structural Composite Materials,” Engineering Materials, Vol 141-143 pp.585-620, 1998.

[12] Cramer D.R. and Taggart, D.F., “Design and Manufacturing of an Affordable Advanced-Composite Automotive Body Structure,” 2002.

[13] Mercedes-Benz SLR McLaren –The Technology, (Cited 2005).

[14] LS-DYNA 970 Keyword Manual, 2005.

[15] National Crash Analysis Center, http://www.ncac.gwu.edu/vml/index.html (Cited 2005).

[16] Anon., “Status of NHTSA Plan for Side Impact Regulation Harmonization and Upgrade,” DOT/NHTSA, March 1999.

APPENDIX

LS-DYNA Composite Modeling Cards

```
*DATABASE_EXTENT_BINARY
$#   NEIPH     NEIPS    MAXINT    STRFLG    SIGFLG    EPSFLG    RLTFLG
ENGFLG
         0         0         0         0         1         1         1
1
$#  CMPFLG    IEVERP    BEAMIP     DCOMP      SHGE     STSSZ    N3THDT
         1         0         0         1         1         1         0

*DATABASE_NODOUT
$#   DT
    0.0001

*PART
$#                                                                HEADING
propbeam
$#     PID     SECID       MID     EOSID      HGID      GRAV    ADPOPT
TMID
         1         1         1         0         0         0         0
0
*SECTION_SHELL
$#   SECID    ELFORM      SHRF       NIP     PROPT        QR     ICOMP
         1         2        0.        13.        0.      -1.         1
$#      T1        T2        T3        T4                MAREA
       3.9       3.9       3.9       3.9                  0.
$#      B1        B2        B3        B4        B5        B6        B7
B8
        0.        80       -80        60       -60        30        0.
30
       -60        60       -80        80        0.
*INTEGRATION_SHELL
$#    IRID       NIP      ESOP
         1        13         0
$#       S        WF       PID
 -0.923077 0.0769231         1
 -0.769231 0.0769231         1
 -0.615385 0.0769231         1
 -0.461538 0.0769231         1
 -0.307692 0.0769231         1
 -0.153846 0.0769231         1
        0. 0.0769231         1
  0.153846 0.0769231         1
  0.307692 0.0769231         1
  0.461538 0.0769231         1
  0.615385 0.0769231         1
  0.769231 0.0769231         1
  0.923077 0.0769231         1

*MAT_ENHANCED_COMPOSITE_DAMAGE
$#     MID        RO        EA        EB        EC      PRBA      PRCA
PRCB
         1  1.58E-09   140000.    10300.        0.      0.27        0.
0.
$#     GAB       GBC       GCA        KF      AOPT
     7200.     5574.     7200.        0.        0.
```

```
$#    TFAIL      ALPH      SOFT      FBRT     YCFAC    DFAILT    DFAILC
EFS
       0.5        0.       0.6        0.        0.        0.        0.
0.
$#      XC        XT        YC        YT        SC      CRIT      BETA
     1096.     1830.      228.       57.       71.       55.        0.

*INITIAL_VELOCITY_RIGID_BODY
$#     PID        VX        VY        VZ       VXR       VYR       VZR
     60002        0.        0.   -13800.        0.        0.        0.

*BOUNDARY_SPC_SET
$#    NSID       CID      DOFX      DOFY      DOFZ     DOFRX     DOFRY
DOFRZ
        12         0         1         1         1         1         1
1


*CONTACT_AUTOMATIC_NODES_TO_SURFACE
$#    SSID      MSID     SSTYP     MSTYP    SBOXID    MBOXID       SPR
MPR
        14        13         2         2         0         0         0
0
$#      FS        FD        DC        VC       VDC    PENCHK        BT
DT
      0.15      0.15        0.        0.        0.         0        0.
0.
$#     SFS       SFM       SST       MST      SFST      SFMT      FSF
VSF
        1.        1.        0.        0.        1.        1.        1.
1.
$#    SOFT    SOFSCL    LCIDAB    MAXPAR     SBOPT     DEPTH     BSORT
FRCFRQ
        0.       0.1        0.        0.        0.        2.        0.
1.
$#  PENMAX    THKOPT              SNLOG      ISYM     I2D3D    SLDTHK
SLDSTF
        0.         0                 0         0         0        0.
0.
```

LS – DYNA Side Impact Modeling Cards

```
*CONTROL_PARALLEL
$#    NCPU    NUMRHS     CONST
         2         0         0

*CONTROL_TIMESTEP
$# DTINIT    TSSFAC      ISDO    TSLIMT     DT2MS      LCTM     ERODE
MSIST
        0.       0.9         0 1.112E-06-1.112E-06         0         0
0

*CONTACT_AUTOMATIC_SINGLE_SURFACE
$#    SSID      MSID     SSTYP     MSTYP    SBOXID    MBOXID       SPR
MPR
       126         0         2         0         2         0         0
0
$#      FS        FD        DC        VC       VDC    PENCHK        BT
DT
       0.2      0.15        0.        0.        0.         0        0.
0.
$#     SFS       SFM       SST       MST      SFST      SFMT       FSF
VSF
        1.        1.        0.        0.        1.        1.        1.
1.
$#    SOFT    SOFSCL    LCIDAB    MAXPAR     SBOPT     DEPTH     BSORT
FRCFRQ
        0.       0.1        0.        0.        0.        2.        0.
1.
$#  PENMAX    THKOPT              SNLOG      ISYM     I2D3D    SLDTHK
SLDSTF
        0.         0                 0         0         0        0.
0.


*LOAD_BODY_Z
$#    LCID        SF    LCIDDR        XC        YC        ZC
         4     9810.         0        0.        0.        0.

*ELEMENT_MASS
       1   11032           0.018
       2   22889          0.0042

*MAT_PIECEWISE_LINEAR_PLASTICITY
$#     MID        RO         E        PR      SIGY      ETAN      FAIL
TDEL
         1  7.85E-09   200000.       0.3      215.        0.     5E+08
0.
$#       C         P      LCSS      LCSR
        0.        0.        5.        0.

*MAT_ELASTIC
$#     MID        RO         E        PR        DA        DB
        90  7.85E-09   200000.       0.3        0.        0.
```

```
*MAT_RIGID
$#     MID        RO         E        PR         N    COUPLE         M
ALIAS/RE
       128 7.8888E-10   200000.       0.3        0.        0.        0.
0.
$#     CMO
        0.
$#      A1        A2        A3        V1        V2        V3
        0.        0.        0.        0.        0.        0.


*MAT_SPRING_GENERAL_NONLINEAR
$#     MID      LCDL      LCDU      BETA       TYI       CYI
       135         2         2        0.        0.        0.

*SECTION_SHELL
$#   SECID    ELFORM      SHRF       NIP     PROPT        QR     ICOMP
         2         2        0.        3.        0.        0.         0
$#      T1        T2        T3        T4                MAREA
      0.82      0.82      0.82      0.82                  0.


*SECTION_BEAM
$#   SECID    ELFORM      SHRF        QR       CST     SCOOR
        92         2        0.        0.        0.        0.
$#       A       ISS       ITT       IRR        SA
     50.27     201.1     201.1     402.1     50.27


*SECTION_SOLID
$#   SECID    ELFORM       AET
       126         0         0


*SECTION_DISCRETE
$#   SECID       DRO        KD        V0        CL        FD
       135         0        0.        0.        0.        0.
$#     CDL       TDL
        0.        0.
        1.

*SET_NODE_LIST
$#     SID       DA1       DA2       DA3       DA4
         3        0.        0.        0.        0.
$#    NID1      NID2
      9106     22736


*DEFINE_CURVE
$#    LCID      SIDR      SCLA      SCLO      OFFA      OFFO    DATTYP
         1         0        0.        0.        0.        0.         0
$#                A1                  O1
                  0.           -0.2413
             0.1005            -0.2413
```

```
*ELEMENT_SEATBELT_ACCELEROMETER
$#  SBACID      NID1      NID2      NID3     IGRAV
         1     26742     26743     26744         0

*CONSTRAINED_SPOTWELD
      4552      5523     9000.     4500.        1.        1.        0.
0.


*MAT_PLASTIC_KINEMATIC
$#     MID        RO         E        PR      SIGY      ETAN      BETA
    2001372.6986E-09 70146.6480.33000001 345.54999 691.09998       0.5
$#     SRC       SRP        FS
        0.        0.        0.


*MAT_HONEYCOMB
$#     MID        RO         E        PR      SIGY        VF        MU
BULK
    2001398.3333E-11 70146.6480.33000001 160.39999    0.0308        0.
0.
$#     LCA       LCB       LCC       LCS      LCAB      LCBC      LCCA
LCSR
      109.      110.      111.      112.        0.        0.        0.
0.
$#    EAAU      EBBU      ECCU      GABU      GBCU      GCAU      AOPT
   1022.82 340.70999 340.70999 435.39001 435.39001 214.24001        0.

$#                                  TSEF      SSEF
                                      0.        0.

*INITIAL_VELOCITY
$#    NSID    NSIDEX     BOXID
       198         0         0
$#      VX        VY        VZ       VXR       VYR       VZR
   -6717.7 -13184.24        0.        0.        0.        0.
```